



Cite this: *Mater. Adv.*, 2023,  
4, 4317

## MXene-based wearable supercapacitors and their transformative impact on healthcare

Siavash Iravani <sup>\*a</sup> and Rajender S. Varma <sup>b</sup>

MXenes have contributed enormously to the development of wearable supercapacitors because of their high surface area, high electrical conductivity, flexibility, hydrophilicity, and good mechanical strength. Such supercapacitors are flexible, lightweight, and can be integrated into textiles, making them ideal for wearable electronics. Various MXene-based composites are introduced with multifunctionality and enhanced conductivity as sensors with wearability and stretchability. However, the design of MXene-based electrodes for wearable supercapacitors still encounters challenges in terms of capacitance, cycling stability, difficulties in synthesis, mechanical flexibility, and integration with other materials. In this context, studies have focused on strategies of deploying composite materials, hybrid approaches, surface modifications, optimization processes, and structural design improvements. Several techniques are introduced to create MXene-based materials with varied deformation capabilities, high capacitance, good cycling stability, and improved mechanical flexibility for wearable supercapacitors. However, some limitations have been circumvented affecting the performance and safety of wearable supercapacitors namely the restacking issues that can reduce their surface area and charge storage capacity, as well as narrow the operating potential range, synthesis challenges, and possible allergenic reactions/toxicity. Wearable technology has emerged as a promising field with applications ranging from fitness tracking to remote monitoring of patients. One key requirement for these devices is a reliable source of power that is both flexible and efficient. MXene-based wearable supercapacitors have shown great potential in the realm of biomedical wearable devices and healthcare monitoring. This perspective article aims to shed light on the significant biomedical applications of MXene-based wearable supercapacitors and their transformative impact on healthcare. In addition, recent developments pertaining to the engagement of MXenes and their composites in designing wearable supercapacitors are deliberated, concluding with the associated main challenges and future directions.

Received 4th July 2023,  
Accepted 23rd August 2023

DOI: 10.1039/d3ma00365e

[rsc.li/materials-advances](http://rsc.li/materials-advances)

### 1. Introduction

Supercapacitors are becoming increasingly important particularly in the development of wearable electronics, including smart watches, sporting equipment, biomedical devices, flexible sensors, and health monitoring patches.<sup>1–3</sup> Supercapacitors can store sufficient energy for wearable electronic devices to enable their operation for extended periods when a harvestable energy source is not available and can be charged using the average current from either an energy harvester or a battery;<sup>4,5</sup> several electrode materials such as  $MnCo_2O_4/NiCo_2O_4$ <sup>6</sup> and reduced graphene oxide (rGO)/polyaniline-gold (Au)- $\gamma$ MnO<sub>2</sub> have been incorporated in the design of supercapacitors.<sup>7</sup>

Indeed, different supercapacitors have been introduced for example electrochemical double-layer, hybrid, pseudo, asymmetric, composite, battery-type, and fiber supercapacitors.<sup>8,9</sup> In this context, the design of flexible supercapacitors for wearable technologies has been growing rapidly owing to their flexibility, fast charging nature, and long-lasting performances. Researchers are exploring the development of self-chargeable flexible solid-state supercapacitors as well as sustainable electronic textiles for wearable electronic functions.<sup>10–12</sup> Among the introduced materials, MXenes have a wide range of unique thermal, optical, mechanical, and electronic properties that make them attractive for various applications, including energy storage, catalysis, drug delivery, tissue engineering, cancer theranostics, sensing, and water purification.<sup>13–16</sup> These two-dimensional (2D) materials with exceptional conductivity and volumetric capacitance as well as tunable properties and chemical versatility are promising candidates for developing supercapacitors. Indeed, the use of MXenes in wearable supercapacitors has garnered immense research interest with

<sup>a</sup>Independent Researcher, W Nazar ST, Boostan Ave, Isfahan, Iran.

E-mail: [siavashira@gmail.com](mailto:siavashira@gmail.com)

<sup>b</sup>Institute for Nanomaterials, Advanced Technologies and Innovation (CxI), Technical University of Liberec (TUL), Studentská 1402/2, Liberec 1 461 17, Czech Republic



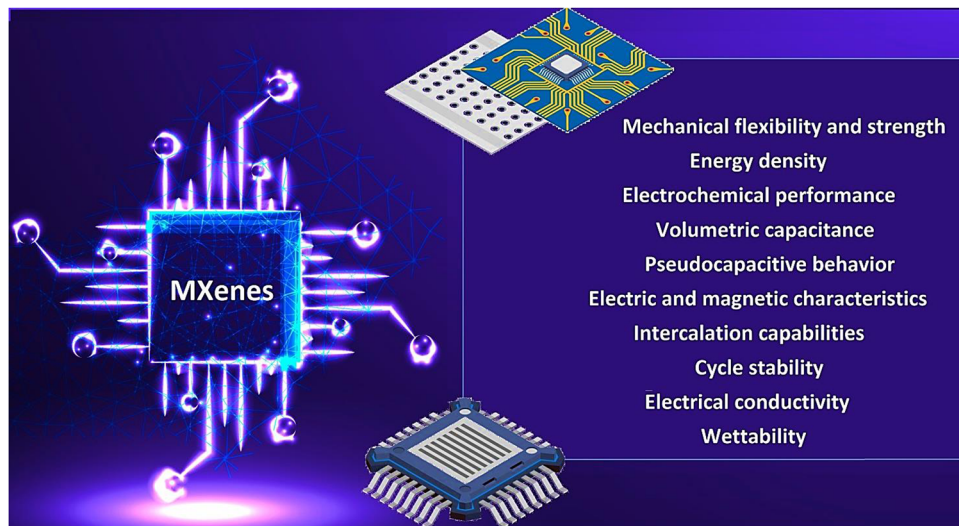


Fig. 1 Important aspects in designing wearable supercapacitors using MXene-based materials.

emphasis on their development encompassing a higher efficiency and performance in wearable electronics (Fig. 1).<sup>17</sup>

Free-standing electrodes with exceptional electrical conductivity along with suitable deformability/durability are crucial in designing flexible electronics especially targeting wearable energy storage devices.<sup>18–20</sup> MXenes with their chemical stability, electrochemical energy benefits, layered structures, high metallic conductivity, and hydrophilicity have been deployed in designing high-performance batteries and supercapacitors.<sup>21–23</sup> However, this new class of 2D materials like other nanomaterials may suffer from drawbacks of restacking and aggregation of individual nanosheets, thus causing poor electrochemical features.<sup>24</sup> For instance, a limited electrolyte-accessible surface area was reported for MXene-based electrodes, producing a low gravimetric capacitance.<sup>25</sup> Consequently, to develop high-performance MXene-based supercapacitors, several tactics have been introduced such as tailoring the ion diffusion resistance by decreasing the MXene mass loading as well as the hybridization of MXenes with other materials (*e.g.*, polymers, metallic oxide/hydroxide, and carbon-based nanomaterials).<sup>26,27</sup> These strategies moderately avoided the restacking of MXene nanosheets with many restacking layers, as exemplified in the case of MXene  $Ti_3C_2T_x$  aerogels with a three-dimensional (3D) architecture.<sup>28</sup>

Various top-down (*e.g.*, HF-based etching) as well as bottom-up (*e.g.*, chemical vapor deposition) strategies have been introduced for fabricating MXenes with energy storage applications, particularly for supercapacitors, micro-supercapacitors/batteries, *etc.* owing to their high electrochemical performance and distinctive layered structures.<sup>29–31</sup> A wide variety of MXene-based composites with excellent volumetric capacitance, high mechanical flexibility, good electrochemical performance, and high energy density have been employed to fabricate supercapacitors.<sup>32,33</sup> Herein, the current trends, main challenges, and future prospects for the deployment of MXenes and their composites in manufacturing wearable supercapacitors are deliberated.

Overall, with recent advancements, MXene-based systems offer an assuring outlook in wearable supercapacitors, and continued investigations are being pursued to address the limitations/challenges that lie ahead concerning their performance and properties.

## 2. MXene-based materials for wearable supercapacitors

MXenes are fascinating 2D materials for wearable supercapacitors owing to their flexibility, durability, and extraordinary electrical conductivity (Table 1); various MXene-based electrode materials have been introduced with suitable electrochemical performances (Table 2). They have the potential to power a variety of wearable devices, including temperature monitoring systems and microcontrollers, and can be integrated into a variety of materials, including textiles and fibers.<sup>34,35</sup> MXenes are endowed with high mechanical flexibility, electrical conductivity, and energy density as well as good electrochemical performance and varied deformation capabilities, which make them ideal candidates for use in wearable supercapacitors/devices that need flexibility and durability along with reliability as efficient power sources.<sup>36,37</sup> However, in MXene-based wearable electronics, there are some important challenges regarding the shrouding issues, possible allergic reactions/toxicity, and integration with other materials. Shrouding may occur when MXene flakes are stacked on top of each other, thus reducing their electrical conductivity and mechanical flexibility.<sup>38</sup> Besides, the integration of MXene-based wearable devices in the human body necessitates ample concern for possible allergic reactions or toxicity. The incorporation of MXenes into other materials may be demanding in terms of the cost of fabrication and the complexity of the involved procedures.<sup>39</sup> Although there has been significant research performed on MXene-based wearable electronics, more explorations ought to



Table 1 Selected examples of MXene-based materials used for the fabrication of wearable supercapacitors

Composites	Applications	Advantages/properties	Ref.
Porous graphene combined with suitable negative electrodes made of MXenes	Wearable asymmetric supercapacitors	<ul style="list-style-type: none"> <li>• High performance with stability and repeatability</li> <li>• High energy density (<math>\sim 107.8 \mu\text{W h cm}^{-2}</math>)</li> <li>• <math>\sim 10000</math> cycles of charge–discharge and <math>\sim 5000</math> cycles of bending</li> </ul>	40
MXene ( $\text{Ti}_3\text{C}_2\text{T}_x$ )/cellulose nanofiber composite films	Wearable supercapacitors; Joule heater	<ul style="list-style-type: none"> <li>• High performance and flexibility</li> <li>• Electrothermal conversion capacity</li> <li>• Complete degradation in hydrogen peroxide solutions</li> <li>• Remarkable tensile strength with high electrical conductivity</li> <li>• Significant capacitance performance (<math>416 \text{ F g}^{-1}</math>, <math>2084 \text{ mF cm}^{-2}</math>)</li> <li>• Excellent mechanical properties and improved flexibility</li> <li>• Maximum energy density was <math>\sim 252 \mu\text{W h cm}^{-2}</math></li> </ul>	41
MXene/bacterial cellulose self-supporting films	3D porous flexible MXene films with superior capacitive performances	<ul style="list-style-type: none"> <li>• Prolonged voltage window of <math>1.6 \text{ V}</math></li> <li>• Significant areal energy density of <math>277.3 \mu\text{W h cm}^{-2}</math></li> <li>• <math>\sim 90\%</math> capacitance retention after <math>30000</math> cycles</li> <li>• The capacitance of the supercapacitor remained at about <math>\sim 74\%</math> even after <math>10000</math> charge/discharge cycles</li> <li>• Stable rechargeable abilities</li> <li>• The areal capacitance could noticeably reach <math>794.2 \text{ mF cm}^{-2}</math> (<math>233.6 \text{ F g}^{-1}</math>)</li> <li>• Excellent volumetric capacitance of <math>\sim 1244.6 \text{ F cm}^{-3}</math> at <math>1 \text{ A g}^{-1}</math></li> <li>• Superb rate capability of <math>\sim 662.5 \text{ F cm}^{-3}</math> at <math>1000 \text{ A g}^{-1}</math></li> <li>• Improved cycling stability with <math>\sim 93.5\%</math> capacitance retention after <math>30000</math> cycles</li> <li>• Significant volumetric energy density (<math>\sim 27.2 \text{ W h L}^{-1}</math>)</li> <li>• Excellent tensile range (strain up to <math>200\%</math>)</li> <li>• Enhanced stability</li> <li>• Outstanding cycling stability (<math>85000</math> cycles) and coulombic efficiency (<math>\sim 99.7\%</math>)</li> </ul>	42
MXene flakes on textile electrode surfaces	Solid-state asymmetric supercapacitors	<ul style="list-style-type: none"> <li>• Significant areal energy density of <math>277.3 \mu\text{W h cm}^{-2}</math></li> <li>• <math>\sim 90\%</math> capacitance retention after <math>30000</math> cycles</li> <li>• The capacitance of the supercapacitor remained at about <math>\sim 74\%</math> even after <math>10000</math> charge/discharge cycles</li> <li>• Stable rechargeable abilities</li> <li>• The areal capacitance could noticeably reach <math>794.2 \text{ mF cm}^{-2}</math> (<math>233.6 \text{ F g}^{-1}</math>)</li> <li>• Excellent volumetric capacitance of <math>\sim 1244.6 \text{ F cm}^{-3}</math> at <math>1 \text{ A g}^{-1}</math></li> <li>• Superb rate capability of <math>\sim 662.5 \text{ F cm}^{-3}</math> at <math>1000 \text{ A g}^{-1}</math></li> <li>• Improved cycling stability with <math>\sim 93.5\%</math> capacitance retention after <math>30000</math> cycles</li> <li>• Significant volumetric energy density (<math>\sim 27.2 \text{ W h L}^{-1}</math>)</li> <li>• Excellent tensile range (strain up to <math>200\%</math>)</li> <li>• Enhanced stability</li> <li>• Outstanding cycling stability (<math>85000</math> cycles) and coulombic efficiency (<math>\sim 99.7\%</math>)</li> </ul>	43
Carbonized MXene/cotton fabrics; MXene ( $\text{Ti}_3\text{C}_2\text{T}_x$ ) flakes	All-solid-state flexible supercapacitors	<ul style="list-style-type: none"> <li>• Excellent volumetric capacitance of <math>\sim 1244.6 \text{ F cm}^{-3}</math> at <math>1 \text{ A g}^{-1}</math></li> <li>• Superb rate capability of <math>\sim 662.5 \text{ F cm}^{-3}</math> at <math>1000 \text{ A g}^{-1}</math></li> <li>• Improved cycling stability with <math>\sim 93.5\%</math> capacitance retention after <math>30000</math> cycles</li> <li>• Significant volumetric energy density (<math>\sim 27.2 \text{ W h L}^{-1}</math>)</li> <li>• Excellent tensile range (strain up to <math>200\%</math>)</li> <li>• Enhanced stability</li> <li>• Outstanding cycling stability (<math>85000</math> cycles) and coulombic efficiency (<math>\sim 99.7\%</math>)</li> </ul>	44
Flexible carbon dot-intercalated MXene film electrodes	All-solid-state symmetric supercapacitors	<ul style="list-style-type: none"> <li>• Excellent volumetric capacitance of <math>\sim 1244.6 \text{ F cm}^{-3}</math> at <math>1 \text{ A g}^{-1}</math></li> <li>• Superb rate capability of <math>\sim 662.5 \text{ F cm}^{-3}</math> at <math>1000 \text{ A g}^{-1}</math></li> <li>• Improved cycling stability with <math>\sim 93.5\%</math> capacitance retention after <math>30000</math> cycles</li> <li>• Significant volumetric energy density (<math>\sim 27.2 \text{ W h L}^{-1}</math>)</li> <li>• Excellent tensile range (strain up to <math>200\%</math>)</li> <li>• Enhanced stability</li> <li>• Outstanding cycling stability (<math>85000</math> cycles) and coulombic efficiency (<math>\sim 99.7\%</math>)</li> </ul>	45
Co@N-carbon nanotube/MXene/carbon nanotube electrode materials	All-solid-state flexible supercapacitors	<ul style="list-style-type: none"> <li>• Excellent gravimetric and areal power density</li> <li>• The capacitance retention above <math>97.7\%</math> for <math>&gt;14000</math> cycles at <math>10 \text{ A g}^{-1}</math></li> <li>• Excellent volumetric specific capacitance (<math>\sim 3.9 \text{ F cm}^{-3}</math> even at a scan rate of <math>1 \text{ V s}^{-1}</math>)</li> <li>• Superb electrochemical activities</li> <li>• Max volumetric energy density was <math>\sim 58.4 \text{ mW h cm}^{-3}</math></li> <li>• The power level of <math>1679.0 \text{ mW cm}^{-3}</math></li> <li>• High cycling stability (<math>\sim 92.4\%</math> retention after <math>10000</math> cycles at <math>10 \text{ A g}^{-1}</math>)</li> <li>• High conductivity for electrons and ions</li> <li>• High specific capacitance (<math>\sim 470 \text{ mF cm}^{-2}</math>)</li> <li>• Significant stretchability up to <math>800\%</math> area strain</li> <li>• More than <math>90\%</math> retention of the initial capacitance after <math>1000</math> stretch/relaxation cycles</li> <li>• Excellent areal capacitance, up to <math>205 \text{ mF cm}^{-2}</math> at <math>50 \text{ mV s}^{-1}</math></li> <li>• Freestanding fiber mats with a high surface area</li> <li>• Notable electrochemical performance; high electrode conductivity</li> <li>• Excellent capacitance</li> <li>• Low internal resistance</li> <li>• Outstanding power density with long-term cycling stability</li> <li>• High flexibility and mechanical strength</li> <li>• High areal specific capacitance and energy storage capacity</li> <li>• Excellent mechanical softness</li> <li>• Superb antioxidation capability</li> <li>• Suitable optoelectronic properties</li> <li>• Suitable sensing all-in-one</li> </ul>	46
Vertically aligned MXene ( $\text{Ti}_3\text{C}_2\text{T}_x$ ) films	High-performance flexible supercapacitors	<ul style="list-style-type: none"> <li>• Excellent gravimetric and areal power density</li> <li>• The capacitance retention above <math>97.7\%</math> for <math>&gt;14000</math> cycles at <math>10 \text{ A g}^{-1}</math></li> <li>• Excellent volumetric specific capacitance (<math>\sim 3.9 \text{ F cm}^{-3}</math> even at a scan rate of <math>1 \text{ V s}^{-1}</math>)</li> <li>• Superb electrochemical activities</li> <li>• Max volumetric energy density was <math>\sim 58.4 \text{ mW h cm}^{-3}</math></li> <li>• The power level of <math>1679.0 \text{ mW cm}^{-3}</math></li> <li>• High cycling stability (<math>\sim 92.4\%</math> retention after <math>10000</math> cycles at <math>10 \text{ A g}^{-1}</math>)</li> <li>• High conductivity for electrons and ions</li> <li>• High specific capacitance (<math>\sim 470 \text{ mF cm}^{-2}</math>)</li> <li>• Significant stretchability up to <math>800\%</math> area strain</li> <li>• More than <math>90\%</math> retention of the initial capacitance after <math>1000</math> stretch/relaxation cycles</li> <li>• Excellent areal capacitance, up to <math>205 \text{ mF cm}^{-2}</math> at <math>50 \text{ mV s}^{-1}</math></li> <li>• Freestanding fiber mats with a high surface area</li> <li>• Notable electrochemical performance; high electrode conductivity</li> <li>• Excellent capacitance</li> <li>• Low internal resistance</li> <li>• Outstanding power density with long-term cycling stability</li> <li>• High flexibility and mechanical strength</li> <li>• High areal specific capacitance and energy storage capacity</li> <li>• Excellent mechanical softness</li> <li>• Superb antioxidation capability</li> <li>• Suitable optoelectronic properties</li> <li>• Suitable sensing all-in-one</li> </ul>	47
Carbon nanotubes/MXene thermoplastic polyurethane hybrid fiber electrodes	All-solid-state fibrous supercapacitors	<ul style="list-style-type: none"> <li>• Excellent volumetric specific capacitance (<math>\sim 3.9 \text{ F cm}^{-3}</math> even at a scan rate of <math>1 \text{ V s}^{-1}</math>)</li> <li>• Superb electrochemical activities</li> <li>• Max volumetric energy density was <math>\sim 58.4 \text{ mW h cm}^{-3}</math></li> <li>• The power level of <math>1679.0 \text{ mW cm}^{-3}</math></li> <li>• High cycling stability (<math>\sim 92.4\%</math> retention after <math>10000</math> cycles at <math>10 \text{ A g}^{-1}</math>)</li> <li>• High conductivity for electrons and ions</li> <li>• High specific capacitance (<math>\sim 470 \text{ mF cm}^{-2}</math>)</li> <li>• Significant stretchability up to <math>800\%</math> area strain</li> <li>• More than <math>90\%</math> retention of the initial capacitance after <math>1000</math> stretch/relaxation cycles</li> <li>• Excellent areal capacitance, up to <math>205 \text{ mF cm}^{-2}</math> at <math>50 \text{ mV s}^{-1}</math></li> <li>• Freestanding fiber mats with a high surface area</li> <li>• Notable electrochemical performance; high electrode conductivity</li> <li>• Excellent capacitance</li> <li>• Low internal resistance</li> <li>• Outstanding power density with long-term cycling stability</li> <li>• High flexibility and mechanical strength</li> <li>• High areal specific capacitance and energy storage capacity</li> <li>• Excellent mechanical softness</li> <li>• Superb antioxidation capability</li> <li>• Suitable optoelectronic properties</li> <li>• Suitable sensing all-in-one</li> </ul>	48
Macroscopic MXene ( $\text{Ti}_3\text{C}_2$ ) ribbon/reduced GO fibers	Fiber-shaped asymmetric supercapacitors	<ul style="list-style-type: none"> <li>• Excellent volumetric specific capacitance (<math>\sim 3.9 \text{ F cm}^{-3}</math> even at a scan rate of <math>1 \text{ V s}^{-1}</math>)</li> <li>• Superb electrochemical activities</li> <li>• Max volumetric energy density was <math>\sim 58.4 \text{ mW h cm}^{-3}</math></li> <li>• The power level of <math>1679.0 \text{ mW cm}^{-3}</math></li> <li>• High cycling stability (<math>\sim 92.4\%</math> retention after <math>10000</math> cycles at <math>10 \text{ A g}^{-1}</math>)</li> <li>• High conductivity for electrons and ions</li> <li>• High specific capacitance (<math>\sim 470 \text{ mF cm}^{-2}</math>)</li> <li>• Significant stretchability up to <math>800\%</math> area strain</li> <li>• More than <math>90\%</math> retention of the initial capacitance after <math>1000</math> stretch/relaxation cycles</li> <li>• Excellent areal capacitance, up to <math>205 \text{ mF cm}^{-2}</math> at <math>50 \text{ mV s}^{-1}</math></li> <li>• Freestanding fiber mats with a high surface area</li> <li>• Notable electrochemical performance; high electrode conductivity</li> <li>• Excellent capacitance</li> <li>• Low internal resistance</li> <li>• Outstanding power density with long-term cycling stability</li> <li>• High flexibility and mechanical strength</li> <li>• High areal specific capacitance and energy storage capacity</li> <li>• Excellent mechanical softness</li> <li>• Superb antioxidation capability</li> <li>• Suitable optoelectronic properties</li> <li>• Suitable sensing all-in-one</li> </ul>	49
MXene ( $\text{Ti}_3\text{C}_2\text{T}_x$ ) electrodes	Ultra-stretchable supercapacitors	<ul style="list-style-type: none"> <li>• Excellent volumetric specific capacitance (<math>\sim 3.9 \text{ F cm}^{-3}</math> even at a scan rate of <math>1 \text{ V s}^{-1}</math>)</li> <li>• Superb electrochemical activities</li> <li>• Max volumetric energy density was <math>\sim 58.4 \text{ mW h cm}^{-3}</math></li> <li>• The power level of <math>1679.0 \text{ mW cm}^{-3}</math></li> <li>• High cycling stability (<math>\sim 92.4\%</math> retention after <math>10000</math> cycles at <math>10 \text{ A g}^{-1}</math>)</li> <li>• High conductivity for electrons and ions</li> <li>• High specific capacitance (<math>\sim 470 \text{ mF cm}^{-2}</math>)</li> <li>• Significant stretchability up to <math>800\%</math> area strain</li> <li>• More than <math>90\%</math> retention of the initial capacitance after <math>1000</math> stretch/relaxation cycles</li> <li>• Excellent areal capacitance, up to <math>205 \text{ mF cm}^{-2}</math> at <math>50 \text{ mV s}^{-1}</math></li> <li>• Freestanding fiber mats with a high surface area</li> <li>• Notable electrochemical performance; high electrode conductivity</li> <li>• Excellent capacitance</li> <li>• Low internal resistance</li> <li>• Outstanding power density with long-term cycling stability</li> <li>• High flexibility and mechanical strength</li> <li>• High areal specific capacitance and energy storage capacity</li> <li>• Excellent mechanical softness</li> <li>• Superb antioxidation capability</li> <li>• Suitable optoelectronic properties</li> <li>• Suitable sensing all-in-one</li> </ul>	50
MXene ( $\text{Ti}_3\text{C}_2\text{T}_x$ )/carbon nanofiber electrodes	Wearable energy storage applications (supercapacitors)	<ul style="list-style-type: none"> <li>• Excellent volumetric specific capacitance (<math>\sim 3.9 \text{ F cm}^{-3}</math> even at a scan rate of <math>1 \text{ V s}^{-1}</math>)</li> <li>• Superb electrochemical activities</li> <li>• Max volumetric energy density was <math>\sim 58.4 \text{ mW h cm}^{-3}</math></li> <li>• The power level of <math>1679.0 \text{ mW cm}^{-3}</math></li> <li>• High cycling stability (<math>\sim 92.4\%</math> retention after <math>10000</math> cycles at <math>10 \text{ A g}^{-1}</math>)</li> <li>• High conductivity for electrons and ions</li> <li>• High specific capacitance (<math>\sim 470 \text{ mF cm}^{-2}</math>)</li> <li>• Significant stretchability up to <math>800\%</math> area strain</li> <li>• More than <math>90\%</math> retention of the initial capacitance after <math>1000</math> stretch/relaxation cycles</li> <li>• Excellent areal capacitance, up to <math>205 \text{ mF cm}^{-2}</math> at <math>50 \text{ mV s}^{-1}</math></li> <li>• Freestanding fiber mats with a high surface area</li> <li>• Notable electrochemical performance; high electrode conductivity</li> <li>• Excellent capacitance</li> <li>• Low internal resistance</li> <li>• Outstanding power density with long-term cycling stability</li> <li>• High flexibility and mechanical strength</li> <li>• High areal specific capacitance and energy storage capacity</li> <li>• Excellent mechanical softness</li> <li>• Superb antioxidation capability</li> <li>• Suitable optoelectronic properties</li> <li>• Suitable sensing all-in-one</li> </ul>	36
MXene/chitin	Wearable and flexible all-solid-state supercapacitors	<ul style="list-style-type: none"> <li>• Excellent volumetric specific capacitance (<math>\sim 3.9 \text{ F cm}^{-3}</math> even at a scan rate of <math>1 \text{ V s}^{-1}</math>)</li> <li>• Superb electrochemical activities</li> <li>• Max volumetric energy density was <math>\sim 58.4 \text{ mW h cm}^{-3}</math></li> <li>• The power level of <math>1679.0 \text{ mW cm}^{-3}</math></li> <li>• High cycling stability (<math>\sim 92.4\%</math> retention after <math>10000</math> cycles at <math>10 \text{ A g}^{-1}</math>)</li> <li>• High conductivity for electrons and ions</li> <li>• High specific capacitance (<math>\sim 470 \text{ mF cm}^{-2}</math>)</li> <li>• Significant stretchability up to <math>800\%</math> area strain</li> <li>• More than <math>90\%</math> retention of the initial capacitance after <math>1000</math> stretch/relaxation cycles</li> <li>• Excellent areal capacitance, up to <math>205 \text{ mF cm}^{-2}</math> at <math>50 \text{ mV s}^{-1}</math></li> <li>• Freestanding fiber mats with a high surface area</li> <li>• Notable electrochemical performance; high electrode conductivity</li> <li>• Excellent capacitance</li> <li>• Low internal resistance</li> <li>• Outstanding power density with long-term cycling stability</li> <li>• High flexibility and mechanical strength</li> <li>• High areal specific capacitance and energy storage capacity</li> <li>• Excellent mechanical softness</li> <li>• Superb antioxidation capability</li> <li>• Suitable optoelectronic properties</li> <li>• Suitable sensing all-in-one</li> </ul>	51
Poly(3,4-ethylenedioxythiophene): poly(styrenesulfonate) (PEDOT:PSS)/MXene/Ag grid ternary hybrid electrodes	Flexible transparent bifunctional capacitive sensors	<ul style="list-style-type: none"> <li>• Excellent volumetric specific capacitance (<math>\sim 3.9 \text{ F cm}^{-3}</math> even at a scan rate of <math>1 \text{ V s}^{-1}</math>)</li> <li>• Superb electrochemical activities</li> <li>• Max volumetric energy density was <math>\sim 58.4 \text{ mW h cm}^{-3}</math></li> <li>• The power level of <math>1679.0 \text{ mW cm}^{-3}</math></li> <li>• High cycling stability (<math>\sim 92.4\%</math> retention after <math>10000</math> cycles at <math>10 \text{ A g}^{-1}</math>)</li> <li>• High conductivity for electrons and ions</li> <li>• High specific capacitance (<math>\sim 470 \text{ mF cm}^{-2}</math>)</li> <li>• Significant stretchability up to <math>800\%</math> area strain</li> <li>• More than <math>90\%</math> retention of the initial capacitance after <math>1000</math> stretch/relaxation cycles</li> <li>• Excellent areal capacitance, up to <math>205 \text{ mF cm}^{-2}</math> at <math>50 \text{ mV s}^{-1}</math></li> <li>• Freestanding fiber mats with a high surface area</li> <li>• Notable electrochemical performance; high electrode conductivity</li> <li>• Excellent capacitance</li> <li>• Low internal resistance</li> <li>• Outstanding power density with long-term cycling stability</li> <li>• High flexibility and mechanical strength</li> <li>• High areal specific capacitance and energy storage capacity</li> <li>• Excellent mechanical softness</li> <li>• Superb antioxidation capability</li> <li>• Suitable optoelectronic properties</li> <li>• Suitable sensing all-in-one</li> </ul>	51



Table 2 Some selected examples of MXene-based supercapacitors and their electrochemical performances

MXene-based electrode materials	Capacitance	Stability	Ref.
Ti <sub>3</sub> C <sub>2</sub> T <sub>x</sub> films	245 F g <sup>-1</sup> at 2 mV s <sup>-1</sup>	100% after 10 000 cycles	52
Alkalized and annealed Ti <sub>3</sub> C <sub>2</sub> T <sub>x</sub> films	1805 F cm <sup>-3</sup> at 1 A g <sup>-1</sup>	98% after 8000 cycles	53
Delaminated Ti <sub>3</sub> C <sub>2</sub> films	633 F cm <sup>-3</sup> at 2 mV s <sup>-1</sup>	95.3% after 10 000 cycles	54
Ti <sub>3</sub> C <sub>2</sub> T <sub>x</sub> films	429 F g <sup>-1</sup> at 1 A g <sup>-1</sup>	89% after 5000 cycles	55
Freeze-dried MXene-10 films	341.5 F g <sup>-1</sup> /922.1 F cm <sup>-3</sup> at 1 A g <sup>-1</sup>	89.3% after 1000 cycles	56
Ti <sub>3</sub> C <sub>2</sub> T <sub>x</sub> -lithium films	892 F cm <sup>-3</sup> at 2 mV s <sup>-1</sup>	100% after 10 000 cycles	57
Modified MXene/holey graphene films	1445 F cm <sup>-3</sup> at 2 mV s <sup>-1</sup>	93% after 10 000 cycles	58
MXene/rGO-5 wt%	1040 F cm <sup>-3</sup> at 2 mV s <sup>-1</sup>	100% after 20 000 cycles	59
MXene-rGO-20 films	329.9 F g <sup>-1</sup> at 5 mV s <sup>-1</sup>	90.7% after 40 000 cycles	60
Layered Ti <sub>3</sub> C <sub>2</sub> /polypyrrole	35.6 mF cm <sup>-2</sup> at 0.3 mA cm <sup>-2</sup>	100% after 10 000 cycles	61
MXene/carbon nanotube-5% films	300 F g <sup>-1</sup> at 1 A g <sup>-1</sup>	92% after 10 000 cycles	62
Ti <sub>3</sub> C <sub>2</sub> T <sub>x</sub> /polyaniline films	272.5 F g <sup>-1</sup> at 1 A g <sup>-1</sup>	71.4% after 4000 cycles	63
Ti <sub>3</sub> C <sub>2</sub> T <sub>x</sub> /PEDOT:PSS	1065 F cm <sup>-3</sup> at 2 mV s <sup>-1</sup>	80% after 10 000 cycles	64
Ti <sub>3</sub> C <sub>2</sub> /FeOOH quantum dot films	115 mF cm <sup>-2</sup> at 2 mA cm <sup>-2</sup>	82% after 3000 cycles	65
MXene/MoO <sub>3</sub>	396 F cm <sup>-3</sup> at 10 mV s <sup>-1</sup>	90% after 5000 cycles	66
MnO <sub>2</sub> /Ti <sub>3</sub> C <sub>2</sub> T <sub>x</sub>	130.5 F g <sup>-1</sup> at 0.2 A g <sup>-1</sup>	100% after 1000 cycles	67
Ti <sub>3</sub> C <sub>2</sub> T <sub>x</sub> /rGO	80 F cm <sup>-3</sup> at 2 mV s <sup>-1</sup>	97% after 10 000 cycles	68
Ti <sub>3</sub> C <sub>2</sub> T <sub>x</sub> films	340 mF cm <sup>-2</sup> at 0.25 mA cm <sup>-2</sup>	82.5% after 5000 cycles	69
Ti <sub>3</sub> C <sub>2</sub> T <sub>x</sub> /rGO	11.6 mF cm <sup>-2</sup> at 0.1 mA g <sup>-1</sup>	100% after 1000 cycles	70
Binder-free Ti <sub>3</sub> C <sub>2</sub> /carbon nanotube films	55.3 F g <sup>-1</sup> at 0.5 A g <sup>-1</sup>	Without capacitance decay over 10 000 cycles	71
Ti <sub>3</sub> C <sub>2</sub> T <sub>x</sub> /polypyrrole/MnO <sub>2</sub>	61.5 mF cm <sup>-2</sup> at 2 mV s <sup>-1</sup>	80.7% after 5000 cycles	72

be conducted on their properties, optimization process, and manufacturing techniques to fully address the potential challenges/limitations of integrating MXenes into wearable technologies.<sup>37</sup>

Free-standing MXene-based electrodes have shown excellent potential in energy storage.<sup>34</sup> Hybrid electrodes could be fabricated from MXenes (Ti<sub>3</sub>C<sub>2</sub>T<sub>x</sub>), rGO, and carbon using a simple template technique, wherein commercial melamine foam has been deployed as a template to form porous architectures of MXene/rGO nanosheets thus introducing nitrogen as a hetero-atom into these nanosheets during the annealing procedure.<sup>34</sup> These electrodes with a gravimetric capacitance of 276 F g<sup>-1</sup> at a current density of 0.5 A g<sup>-1</sup> could be assembled into supercapacitors, and they exhibit stable electrochemical activity at various compressive strains. When the foam electrodes were coated with a polyvinyl alcohol-H<sub>2</sub>SO<sub>4</sub> gel electrolyte, they could be compressed into flexible films at ~80% of compression. The assembly of the supercapacitors with the film provided stable capacitance under various modes of deformations, including bending and twisting.<sup>34</sup> Zhou *et al.*<sup>41</sup> introduced high-performance composite films created from MXene nanosheets and cellulose nanofibers through an electrostatic self-assembly technique persuaded by polyethyleneimine. These films with suitable electrothermal conversion capacities exhibited superb flexibility and tensile strength along with stable electrical conductivity owing to the nacre-like microstructure of MXenes “bricks” and cellulose nanofibers “mortars” interlocked by polyethyleneimine through hydrogen bonding and electrostatic interactions. They were employed in designing symmetric quasi-solid-state supercapacitors with a capacitance of 93.9 mF cm<sup>-2</sup> at a current density of 0.1 mA cm<sup>-2</sup>. Such film composites with high performance mechanical robustness, and flexibility ought to be further explored to acquire environmentally-friendly energy storage and conversion devices.<sup>41</sup> In another study aimed at supercapacitors, flexible electrode materials with

excellent electrical conductivity were constructed through a vacuum-assisted filtration technique utilizing MXene (Ti<sub>3</sub>C<sub>2</sub>T<sub>x</sub>)/vanadium pentoxide (V<sub>2</sub>O<sub>5</sub>) hybrid films (Fig. 2).<sup>73</sup> The nanofibers of V<sub>2</sub>O<sub>5</sub> were introduced for suppressing the self-stacking occurrence in MXene nanosheets and for simultaneously regulating the thickness of MXene/V<sub>2</sub>O<sub>5</sub> films. The electrode films displayed improved capacitive performance (~319.1 F g<sup>-1</sup>, 0.5 A g<sup>-1</sup>) with a cycling stability of ~70.4% after 5000 cycles at 3 A g<sup>-1</sup>. Such flexible MXene-based electrodes with unique electrochemical properties still need to be additionally looked into for attaining high-performance all-solid supercapacitors for next-generation wearable devices.<sup>73</sup>

Controllable 3D architectures were developed using 2D MXene nanosheets through a simple freeze-induced co-assembly technique, allowing the disparate integration of MXenes into the directive heterogeneities for customizing 3D aerogels with multifunctionality and structural integrity.<sup>74</sup> The functionalized cellulose nanocrystals, serving as structural and framework modifiers, were adopted to produce multilevel MXene 3D aerogels across multiple length scales, thus offering mechanical robustness and multifunctionality (Fig. 3). These aerogels exhibited excellent electrochemical attributes with a high-rate capacity and temperature-invariant super-elasticity (0–150 °C) owing to the high ion pathway from the low-tortuosity topology. The constructed MXene quasi-solid-state supercapacitors displayed superb electrochemistry with an energy density of ~38.5 μW h cm<sup>-2</sup> as well as excellent cycle stability of ~86.7% after 4000 cycles. Such structures with a high photo-response capacity can also be applied as integrated photodetectors. The MXene 3D aerogels have been deployed in designing smart and self-powered lightweight wearable electronic devices to monitor various human motions, thus exploiting their mechanically self-adaptive resilience.<sup>74</sup> In another study, cobalt-metal organic framework structures were developed on a MXene-carbon nanofiber mat with high flexibility and electroconductivity.<sup>75</sup>



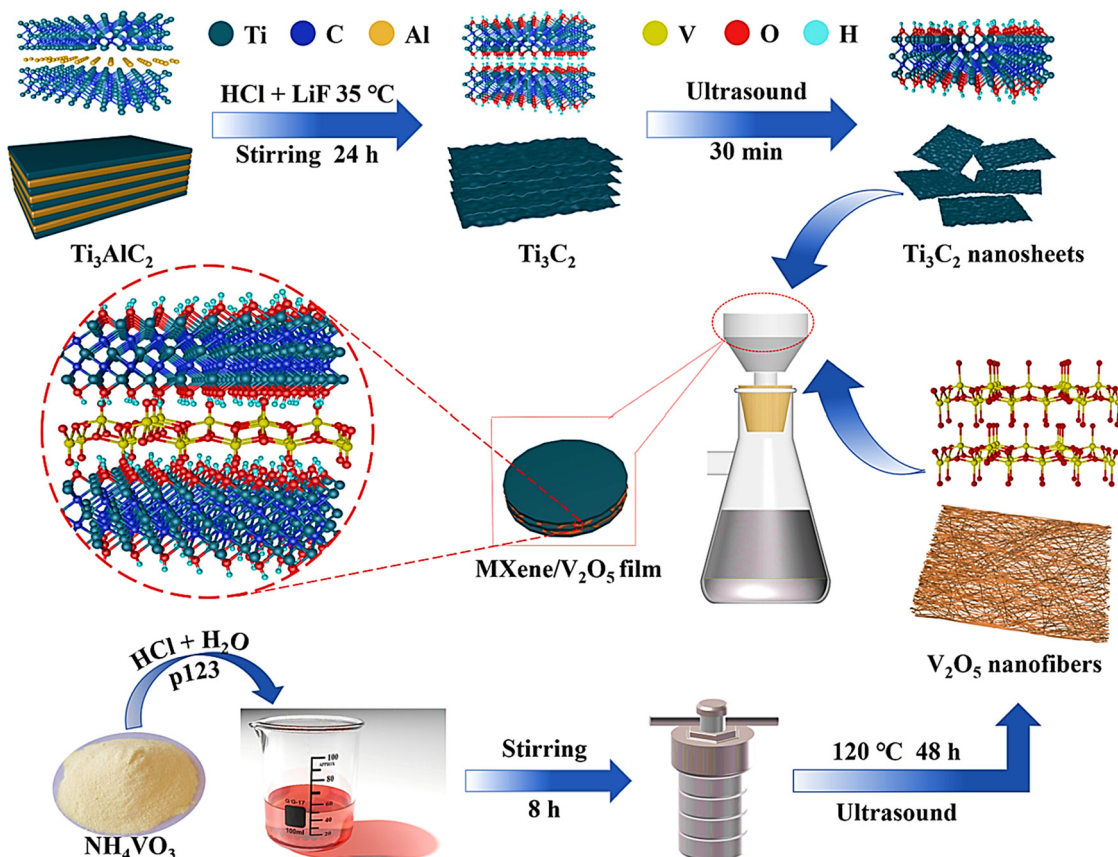


Fig. 2 The preparative process for MXene/V<sub>2</sub>O<sub>5</sub> hybrid films via a vacuum-assisted filtration technique. Reproduced with permission from ref. 73. Copyright 2023 Elsevier.

The resulting composites were used in designing capacitive- and battery-type functional multi-component electrodes to obtain wearable hybrid quasi-solid-state supercapacitors with high mechanical flexibility and performance. As a result, these electrodes with an operating voltage window of 1.5 V, bringing an energy density of 72.5 W h kg<sup>-1</sup> at a power density of 832.4 W kg<sup>-1</sup> with long-term stability ( $\sim 90.36\%$  capacitance retention), signify great potential in the construction of different smart wearable devices.<sup>75</sup>

One of the important challenges has been to identify controllable and efficient tactics for fabricating binder-free MXene-based electrodes to generate MXene-based wearable flexible supercapacitors.<sup>76,77</sup> In one study, a binder-free MXene ( $\text{Ti}_3\text{C}_2\text{T}_x$ )-based system was created with controllable mass loading and abridged agglomeration on the nickel foam and wearable flexible fabric substrates using an altered electro-phoretic deposition technique (Fig. 4).<sup>78</sup> Such binder-free electrodes exhibited a significant capacitance of  $\sim 140$  F g<sup>-1</sup> in an alkaline electrolyte with stable cycling activity and improved rate performance; no capacitance loss could be detected even after 10 000 cycles. These MXene films with reduced agglomeration, optimized pore-size distribution, and enhanced electronic conductivity displayed enhancement in the accessibility to electrolyte ions, which resulted in full engagement of the MXene nanoflake surfaces.<sup>78</sup> In addition, a textile-based

electrochemical supercapacitor has been developed using MXene ( $\text{Ti}_3\text{C}_2\text{T}_x$ ), which can be applied for wearable electronics,<sup>35</sup> and the resulting supercapacitor operated in a 6 V voltage window, and could deliver an energy density of 0.401 mW h cm<sup>-2</sup> at a power density of 0.248 mW cm<sup>-2</sup>. This MXene textile supercapacitor could power a temperature monitoring system needing excessive current densities with wireless data transmission to a receiver for 96 min, thus revealing its great potential for applications in biomedical monitoring devices.<sup>35</sup>

To overcome the limitations of traditional energy storage systems in satisfying the performance requirements for flexible electronics, the electrodes have been fabricated from MXene ( $\text{Ti}_3\text{C}_2$ ) and 1T-Phase WS<sub>2</sub> nanosheets to develop flexible asymmetric supercapacitors on polyester/cellulose blend cloth substrate.<sup>79</sup> The resulting 2D electrodes exhibited high performance, flexibility and cyclic stability, providing wearable supercapacitors with excellent potential in healthcare such as bio-monitoring sensing applications.<sup>79</sup> Li *et al.*<sup>80</sup> introduced a MXene-coated cotton fabric-based personal body thermal management system with suitable water vapor and air permeability as well as wear resistance and wash stability. The MXene-coated cotton fibers exhibited excellent electron conductivity ( $\sim 197$  mS cm<sup>-2</sup>), showing outstanding heating efficiency (up to 100 °C within 10 s under the low applied potential of 3 V).

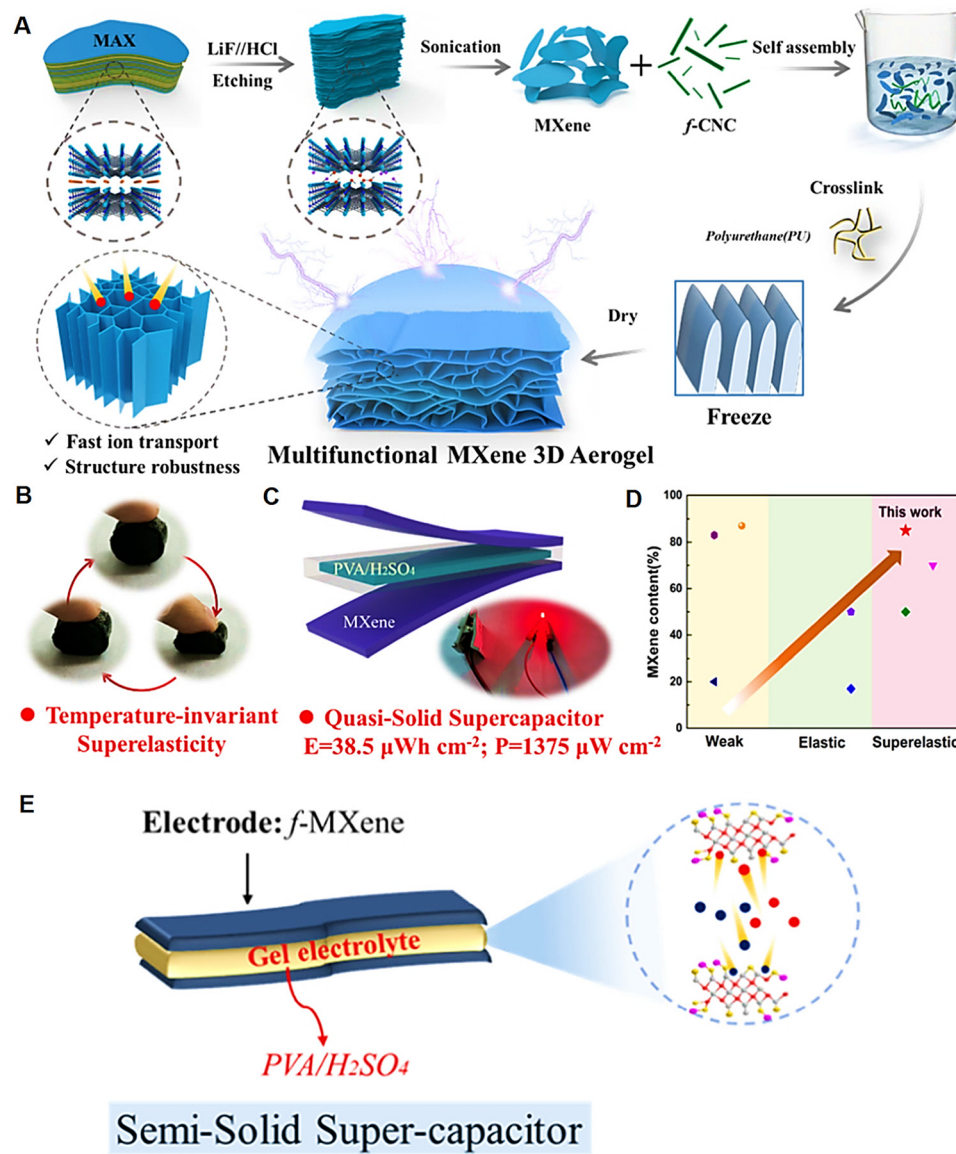


**Fig. 3** (A) The preparative process for MXene 3D aerogels through a simple cryo-assembly technique. (B) MXene aerogels with temperature-invariant superelasticity properties. (C) The designed MXene-based supercapacitor, and (D) the curve of the mechanical property vs. MXene loading. (E) An MXene solid supercapacitor with its sandwich structure, showing excellent energy storage properties. Reproduced with permission from ref. 74 Copyright 2021 American Chemical Society.

These materials could be employed as the electrodes of supercapacitors, providing significant areal specific capacitance ( $\sim 208 \text{ mF cm}^{-2}$ ) at a scan rate of  $5 \text{ mV s}^{-1}$ . As a result, the symmetric supercapacitors provided excellent energy density ( $2 \text{ } \mu\text{Wh cm}^{-2}$ ) along with the power density of  $\sim 5.3 \text{ mW cm}^{-2}$ , thus signifying the great potential of such supercapacitors in wearable electronics.<sup>80</sup>

MXene/polyvinyl alcohol fibers were prepared *via* a simple wet-spinning technique, showing suitable stretchability and notable electrochemical characteristics.<sup>81</sup> The fiber-based supercapacitors with excellent gravimetric capacitance ( $\sim 119.3 \text{ F g}^{-1}$ ) and areal capacitance ( $\sim 130.9 \text{ mF cm}^{-2}$ ) displayed robust durability in multiple mechanical states along with the steady electrochemical mode after stretching, offering great potential for developing

efficient energy storage devices.<sup>81</sup> Similarly, Yang *et al.*<sup>82</sup> fabricated MXene-based fibers using a wet-spinning assembly technique exploiting the synergistic effect between liquid crystals of GO and MXene sheets. Consequently, the integrated fiber-constructed supercapacitors exhibited enhanced electrical conductivity ( $2.9 \times 10^4 \text{ S m}^{-1}$ ) as well as superb volumetric capacitance ( $586.4 \text{ F cm}^{-3}$ ).<sup>82</sup> Hu *et al.*<sup>83</sup> created all-solid-state flexible fiber-shaped supercapacitors utilizing MXenes ( $\text{Ti}_3\text{C}_2\text{T}_x$ ) and silver-plated nylon fibers. Accordingly, the chemically cross-linked polyvinyl alcohol-H<sub>2</sub>SO<sub>4</sub> hydrogels were employed as solid-state electrolytes, which assured the mechanical strength and structural integrity of these supercapacitors encompassing excellent areal capacitance ( $\sim 328 \text{ mF cm}^{-2}$ ) along with high flexibility/cyclability. The capacitance retention



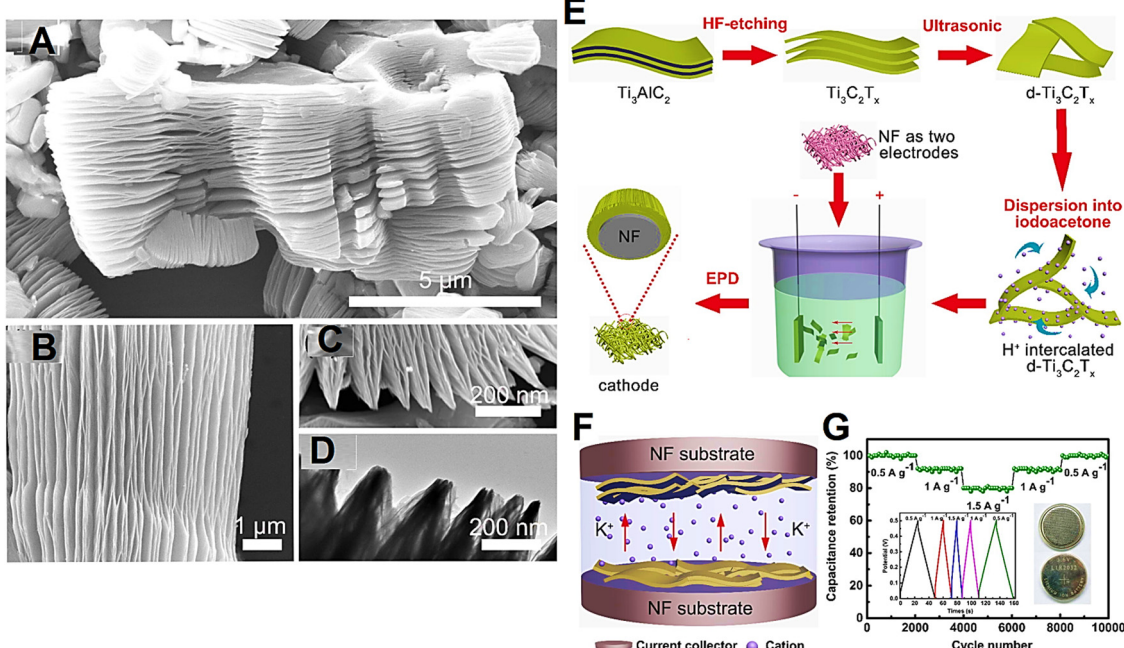


Fig. 4 (A)–(C) Scanning electron microscopy (SEM) and (D) transmission electron microscopy (TEM) images of MXene nanoflakes at different magnifications. (E) The preparative process of MXene-based electrode films. (F) The mechanism of the charge–discharge procedure in the symmetric coin cell. (G) Cycling performance of the symmetric coin cell with two constructed d-Ti<sub>3</sub>C<sub>2</sub>T<sub>x</sub> film electrodes (mass loading 5.6 mg for each electrode) at current densities 0.5, 1 and 1.5 A g<sup>-1</sup>, respectively. The galvanostatic charge–discharge curves (2000th–10 000th cycles) with photographs of the coin cell are displayed. Reproduced with permission from ref. 78 Copyright 2017 Elsevier.

could persist >80% under different deformation modes of knotting, twisting, and bending.<sup>83</sup>

Despite recent advancements in the field of wearable electronics, the fabrication of electronic textiles with the benefits of multifunctionality, breathability, high conductivity, and elasticity still encounters significant hurdles.<sup>84–86</sup> In one study, a chemical polymerization and coating tactic was deployed for fabricating interconnected networks of polyaniline nanoarrays and MXenes on the fiber surfaces.<sup>87</sup> The resulting elastic polyaniline nanoarrays/MXene textiles exhibited low electrical resistance, which could be utilized to prepare all-solid-state supercapacitors with a high specific capacitance (~647 mF cm<sup>-2</sup>) and energy density (~8.08 μWh cm<sup>-2</sup>). These highly conductive smart fabrics with their high sensitivity can be deployed in the creation of wearable sensors for accurate detection of human motions, thus paving the way for designing high-performance textile-based wearable electronic devices.<sup>87</sup> Zheng *et al.*<sup>88</sup> developed conducting polymer/MXene (Ti<sub>3</sub>C<sub>2</sub>T<sub>x</sub>) textiles using a vapor phase polymerization and spray-coating technique. Such textiles with a low sheet resistance of 3.6 Ω sq<sup>-1</sup> exhibited excellent electrochemical, strain sensing, and Joule heating performances as well as suitable electromagnetic interference shielding potential. The assembled all-solid-state fabric supercapacitors with an ultrahigh specific capacitance of 1000.2 mF cm<sup>-2</sup> can be exploited in designing multifunctional wearable electronic devices. The modified MXene-based fabrics displayed an outstanding Joule heating function of ~193.1 °C at an applied voltage of 12 V, along with the significant electromagnetic interference shielding effectiveness of ~36.62 dB.<sup>88</sup>

To fabricate high-performance flexible supercapacitors with diverse configurations, researchers have employed MXene (Ti<sub>3</sub>C<sub>2</sub>) nanosheets (the electrodes) and organic ionic conductor-induced hydrogels (the electrolytes);<sup>89</sup> preparations comprise sandwich, twisted fiber, and interdigitated configurations. Accordingly, the sandwich configuration displayed a specific capacitance of 307 F g<sup>-1</sup> at a low current density (~0.8 A g<sup>-1</sup>), while the interdigitated configuration had an excellent specific capacitance of 92 F g<sup>-1</sup> at a high current density (10 A g<sup>-1</sup>) besides exhibiting long-term stable cyclability (~10<sup>4</sup> cycles) and mechanical flexibility.<sup>89</sup> Notably, the improvement in performance of these supercapacitors was primarily due to the presence of the narrow distance between the electrodes reducing the ion transport resistance and fastening the ion diffusion. After being connected in series, the MXene-based flexible supercapacitors could be deployed to power up small commercial electronic gadgets, offering great potential in powering wearable electronic devices.<sup>89</sup> In view of the importance of wearable fiber-based electronics particularly in self-powering healthcare monitoring, wearable carbon fiber-based asymmetric supercapacitors have been designed using additive-free aqueous MXene/polyaniline inks. The supercapacitors could be deployed for powering wearable pressure sensors, monitoring motions and pulse signals.<sup>90</sup> Such wearable and fiber-based self-powered sensors with the advantages of simplicity and cost-effectiveness are representatives of this emerging technology that has the potential to revolutionize personalized healthcare and telemedicine.<sup>91</sup>

The exploration of new materials and designs to improve the performance and efficiency of all-solid-state photothermal

supercapacitors is being pursued as they can deliver electrochemical energy over a wide range of temperatures, with advantages of mechanical robustness and flexibility. Additionally, some research has focused on enhancing the solar energy harvest of photothermal supercapacitors to improve their performance.<sup>92</sup> Notably, the generation of MXene-based all-solid-state supercapacitors encompassing mechanical robustness, geometrical flexibility, and significant energy density is still a crucial lingering issue, particularly in designing electronic devices with wearability and portability due to the significant restacking in the system and lack of robust interactions in individual MXene nanosheets.<sup>93</sup> Cai *et al.*<sup>93</sup> developed MXenes inspired by the mortar and brick structure of nacre, showing an enhanced photothermal conversion performance, excellent mechanical strength (78.3 MPa), and flexibility. In this study, one-dimensional cellulose nanofibrils and 2D tin(IV) sulfide ( $\text{SnS}_2$ ) were utilized as building blocks to assemble a structure-layered 3D architecture and efficient intercalator for overwhelming the recalcitrant restacking of nanosheets. Accordingly, the highly flexible all-solid-state photothermal supercapacitor exhibited a significant energy density of  $6.7 \mu\text{W h cm}^{-2}$  and  $\sim 91.5\%$  capacitance retention after 4000 cycles as well as superb cyclability ( $> 90\%$  capacitance retention after 500 times of folding/unfolding).<sup>93</sup>

At the moment, the engagement of micro-supercapacitors for powering the integrated wearable monitoring systems has

witnessed significant progress.<sup>94</sup> In one study, the integration of MXene electrochemical micro-supercapacitors with a triboelectric nanogenerator was performed to design a self-powered wearable monitoring system (Fig. 5).<sup>95</sup> Accordingly, the micro-supercapacitor could deliver a capacitance of  $23 \text{ mF cm}^{-2}$  (the capacitance retention was  $\sim 95\%$  after 10 000 charge-discharge cycles), with the max output power of the triboelectric nanogenerator being  $7.8 \mu\text{W cm}^{-2}$ . The power system could be constantly charged through the regular human motion ( $\sim 5 \text{ Hz}$ ) with no noticeably discernible current leakage. Such micro-supercapacitors can be applied in designing various electronic devices or sensors.<sup>95</sup>

The design of metal ion hybrid micro-supercapacitors is one of the noteworthy topics in energy storage domain.<sup>96,97</sup> In one study, zinc-ion hybrid micro-supercapacitors were designed using MXene ( $\text{Ti}_3\text{C}_2\text{T}_x$ )-based electrodes as capacitor-type anodes and  $\text{V}_2\text{O}_5$ -based electrodes as battery-type cathodes (Fig. 6). These supercapacitors exhibited improved electrochemical features, with a high capacitance of  $129 \text{ mF cm}^{-2}$  under  $0.34 \text{ mA cm}^{-2}$  along with a significant energy density of  $\sim 48.9 \mu\text{W h cm}^{-2}$  at  $673 \mu\text{W cm}^{-2}$ ; the cycle stability was also acceptable ( $\sim 77\%$  capacitance after 10 000 cycles).<sup>96</sup>

Benefiting from excellent metal-like conductivity, hydrophilic surfaces, and mechanical attributes of MXenes, various electrode materials have been designed with electrochemical energy applications. However, there are still challenges for

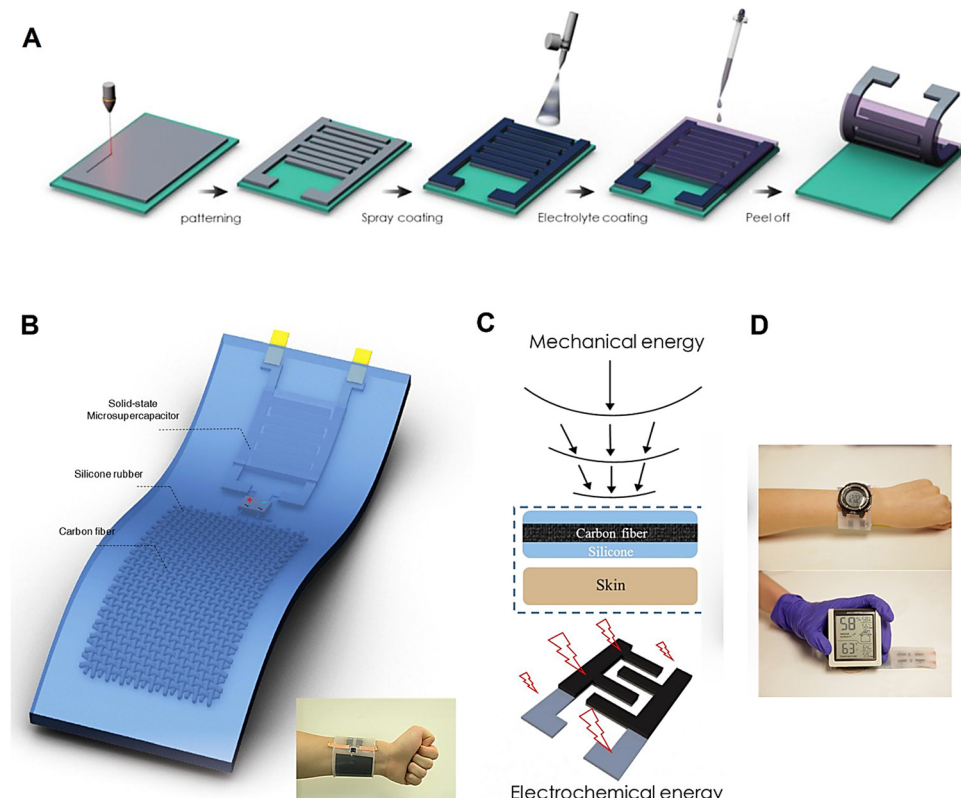


Fig. 5 (A) The preparative process for MXene ( $\text{Ti}_3\text{C}_2\text{T}_x$ )-based electrochemical micro-supercapacitors. (B) The design of wearable self-charging power systems. (C) The mechanism of electricity generation for charging the micro-supercapacitors. (D) The engagement of the micro-supercapacitor to drive a digital watch and commercial temperature-humidity meter. Reproduced with permission from ref. 95 Copyright 2018 Elsevier.



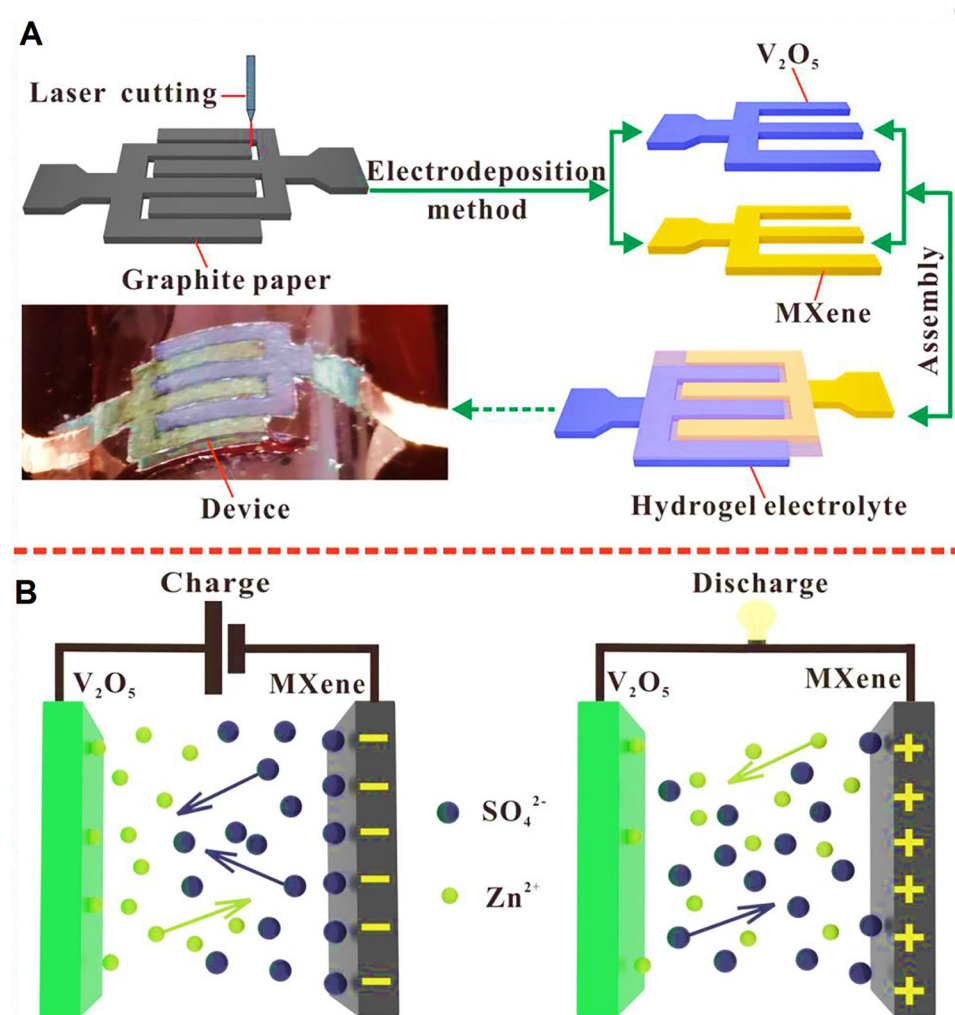


Fig. 6 (A) The design of high-performance flexible Zn-ion hybrid micro-supercapacitors using the MXene anode and  $\text{V}_2\text{O}_5$  cathode. (B) The related mechanism of energy storage using flexible Zn-ion hybrid micro-supercapacitors (the states of charge and discharge). Reproduced with permission from ref. 96 Copyright 2021 Elsevier.

incorporating stiff MXene nanosheets into deformable energy storage devices due to significant mechanical stiffness along with the poor inter-sheet interaction; thus, there is vital demand in designing electrodes to withstand large mechanical deformations without the loss of their electrochemical performances.<sup>22,98</sup> To circumvent these challenges, Chang *et al.*<sup>22</sup> introduced a mechanically driven assembly tactic for fabricating high-performance MXene-based supercapacitors with stretchability, bendability, and excellent mechanical stability (Fig. 7). This approach comprised adjusted crumpling of MXene hybrid nano-coatings to acquire high-areal-capacitance electrodes. Additionally the nano-coating process undergoes multigenerational shrinkage pathways to attain multi-scale MXene structures serving as electrochemical electrodes. After transferring these MXene structures on soft elastomers, the electrodes of MXene/elastomer could be acquired for designing stretchable and bendable high-performance supercapacitors.<sup>22</sup>

### 3. Healthcare applications

#### 3.1. Wearable health monitoring

MXene-based supercapacitors with their flexibility, lightweight, and biocompatibility can be applied as ideal power sources for wearable health monitoring devices. These wearable devices can continuously track physiological parameters such as heart rate, blood pressure, temperature, and respiratory rate, enabling the real-time health monitoring and early detection of potential health risks. In addition, integrated self-powered devices based on MXenes have emerged as important themes in the literature, particularly in the field of wearable devices.<sup>17</sup> For instance, a self-powered triboelectric MXene-based 3D-printed wearable physiological bio-signal sensing system was developed for on-demand, wireless, and real-time health monitoring.<sup>99</sup> The system encompassed power-efficient triboelectric nano-generators, highly sensitive pressure sensors, and multifunctional circuitry. The core material used was MXene, which possesses distinctive electro-negative and conductive characteristics and can be 3D-printed.

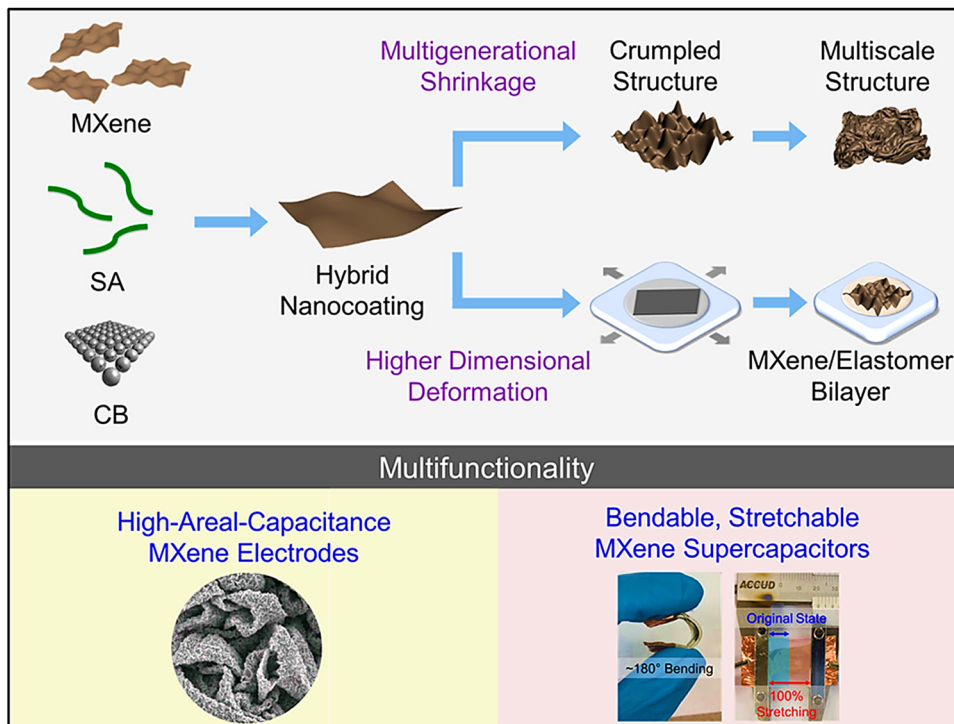


Fig. 7 The preparative process for multi-scale MXene structures and MXene/elastomer bilayers in designing bendable and stretchable supercapacitors. Reproduced with permission from ref. 22 Copyright 2018 American Chemical Society.

MXenes have been combined with a skin-like substrate called styrene-ethylene-butylene-styrene, exhibiting positive triboelectric properties and high stretchability. This self-powered physiological sensing system demonstrated a power output of  $\sim 816.6 \text{ mW m}^{-2}$  and sensitivity of  $\sim 6.03 \text{ kPa}^{-1}$ , with a low detection limit of  $\sim 9 \text{ Pa}$  and a fast response time of  $\sim 80 \text{ ms}$ . These features have enabled continuous monitoring of radial artery pulse waveforms without the need for external power. The system also showcased continuous, on-demand, fully self-powered radial artery pulse monitoring, as well as wireless data and power transmission through near-field communication.<sup>99</sup> In another study, multitasking aqueous printable MXene inks were developed as an additive-free high-capacitance electrode, sensitive pressure-sensing material, highly conducting current collector, metal-free interconnector, and conductive binder.<sup>100</sup> These MXene inks could be directly screen printed to fabricate MXene-based micro-supercapacitors and lithium-ion micro-batteries on various substrates. The fabricated micro-supercapacitors exhibited an ultrahigh areal capacitance of  $1.1 \text{ F cm}^{-2}$ , and when serially connected, they achieved a record voltage of  $60 \text{ V}$ . The quasi-solid-state lithium-ion micro-batteries displayed a robust areal energy density of  $154 \text{ } \mu\text{W h cm}^{-2}$ . Besides, an all-flexible self-powered integrated system was demonstrated on a single substrate using the multitasking MXene inks. This integrated system seamlessly integrated a tandem solar cell, the lithium-ion micro-battery, and an MXene hydrogel pressure sensor. Notably, this integrated system presented exceptional sensitivity to body movements, with a fast response time of  $35 \text{ ms}$ . Thus, the

development of this kind of multipurpose MXene ink paves the way for powering future smart medical devices.<sup>100</sup> While the potential of MXene-based self-powered devices in wearable technology is promising, several challenges need to be addressed. These include optimizing the performance and stability of MXene materials, improving the scalability of 3D-printing techniques, and ensuring the long-term reliability in real-world conditions.

### 3.2. Bioelectronic medical devices

MXene-based supercapacitors can play a pivotal role in powering bioelectronic medical devices, developing the treatment and monitoring of various medical conditions.<sup>17,101,102</sup> For instance, flexible multichannel electrode arrays were developed utilizing MXenes, wherein the electrodes were created in both planar and 3D forms. Accordingly, they were applied to the skin of volunteers for various purposes, including electroencephalography for recording brain activity, electromyography for measuring muscle activation, electrocardiography for monitoring heart activity, and electrooculography for mapping the eye movement. In addition, the electrode arrays were successfully implanted in pigs and rats for intraoperative monitoring and brain stimulation, while also demonstrating compatibility with magnetic resonance and computed tomography imaging. These flexible interfaces have potential for clinical applications in multi-scale epidermal sensing and neuro-modulation.<sup>101</sup> Notably, by integrating MXene-based supercapacitors into implantable devices, such as neuro-stimulators or drug delivery systems, they facilitate precise and localized therapies. These devices can be wirelessly controlled and powered by the



supercapacitors, resulting in targeted treatments for chronic pain, neurological disorders, and even cancer.<sup>103,104</sup> In one study, a lightweight, thin, stretchable, and wet-adhesive all-hydrogel micro-supercapacitor was successfully developed. This remarkable supercapacitor implant exhibited a high areal capacitance, and was not only biocompatible but also specifically designed for localized therapies.<sup>103</sup>

### 3.3. Prosthetics and rehabilitation

MXene-based wearable supercapacitors offer tremendous potential in the field of prosthetics and rehabilitation.<sup>38</sup> By harnessing their flexibility and lightweight nature, these supercapacitors can power advanced prostheses, enabling amputees to regain dexterity, mobility, and the sense of touch. The improved power delivery and enhanced functionality of such devices can significantly enhance the quality of life for individuals with limb loss or physical disabilities. The high energy storage capacity of MXene-based supercapacitors allows for a longer-lasting power supply, which is crucial for prosthetics and rehabilitation devices requiring sustained operation. Besides, the flexibility of these supercapacitors enables comfortable and unobtrusive integration into wearable devices, ensuring a better user experience.<sup>105</sup>

### 3.4. Remote patient monitoring

With the advent of telemedicine and remote patient monitoring, MXene-based wearable supercapacitors can overcome challenges/limitations associated with traditional power sources, enabling seamless and continuous health monitoring.<sup>106,107</sup> These supercapacitors can power wearable devices that transmit vital health data to healthcare professionals in real-time, allowing for remote diagnostics, personalized care, and timely intervention, particularly in underserved areas or during emergencies.<sup>106,108</sup> For instance, the use of MXene waste materials to develop wearable devices has been reported, providing promising platforms for remotely monitoring real-time physiological signals to assess human health status.<sup>106</sup>

### 3.5. Smart textiles and wearable integration

The versatility of MXene-based wearable supercapacitors extends into the realm of smart textiles and wearable integration.<sup>35</sup> These supercapacitors can be seamlessly integrated into clothing, fabrics, or even bandages, providing an uninterrupted power supply for various wearable devices. This assimilation can enable applications like energy-harvesting garments, smart clothing with biometric sensing capabilities, and wound dressings that monitor healing progress.<sup>109,110</sup> In one study, a waterproof and breathable smart textile was developed using a multiple core-shell structure, by decorating MXene onto a polydopamine modified surface, followed by a polydimethylsiloxane coating.<sup>111</sup> The MXene wrapping shaped a conductive network within the fibers, while the polydimethylsiloxane provided protection against oxidation and imparted superhydrophobicity, resulting in corrosion resistance. The smart textile exhibited exceptional and long-lasting photothermal and electrothermal conversion performances. Besides, the textile offered sensitive and stable strain

sensing capabilities as well as temperature sensing potential, with a high thermal coefficient of resistance.<sup>111</sup> These smart textile devices show great promise for future applications in all-in-one wearable electronics. In addition, yarn supercapacitors have revealed great promises to afford power for the next-generation of textile electronic devices, as exemplified in the case of polyester@MXene nanofiber-based yarn electrodes. Nonetheless, several crucial factors such as manufacturability, mechanical strength, flexibility, and electrochemical features need to be contemplated to achieve electroactive yarns with all-textile properties.<sup>112</sup> In one study, MXene-based yarn supercapacitors were designed with high performance and stability even under bending or twisting. Such MXene-based supercapacitors can be incorporated as high-performance flexible power sources to operate miniaturized and wearable electronic devices.<sup>32</sup>

## 4. Challenges and perspectives

MXenes with their unique properties such as hydrophilicity, mechanical flexibility and robustness, high specific capacitance, metallic conductivity, and ease of processability in solution have been studied in designing flexible wearable energy storage devices.<sup>113,114</sup> For instance, MXene nanosheets could be deployed for fabricating smart wearable self-powered health monitoring systems, as exemplified in the case of flexible solid-state supercapacitors constructed from MXene/polyamide films with improved mechanical features and specific capacitance.<sup>106</sup> The importance of freestanding and flexible electrodes has prompted extensive research explorations to help address the problems such as the noteworthy trade-off between mechanical flexibility and electrochemical activity of electrodes. Thus, not surprisingly, the design of flexible and freestanding multicomponent hybrid electrodes exploiting MXenes with enhanced electrochemical features is one of the prominent enduring research areas.<sup>75,115</sup> In addition, carbon cloth is a promising alternative for designing all-solid-state flexible supercapacitors, and is capable of fulfilling all the requirements to realize lightweight, conductive, corrosion-resistant flexible supercapacitors substrates.<sup>116</sup> Nevertheless, one of the vital challenges relates to difficulty in adherence because of the hydrophobic surfaces wherein, MXene flakes can be applied for coating the surfaces of modified carbon cloth to improve their physicochemical properties, thus paving the way for enhancing the performance of supercapacitors through the oxygen plasma and chemical alteration. Accordingly, these flexible MXene/carbon cloth electrodes have shown a higher areal capacitance with enhanced capacitance retention.<sup>116</sup>

Several innovative supercapacitors have been designed based on the intrinsic metallic conductivity of MXene sheets along with their oriented stacking structure, as illustrated in the case of fiber-shaped asymmetric supercapacitors.<sup>48</sup> In view of the significant volumetric capacitance, electro-chromic behavior, high electronic conductivity, and optical transparency, MXenes have been exploited for developing smart fibers with



multipurpose performances for wearable and portable electronics.<sup>117,118</sup> For example, high-performance smart fibers with appropriate applicability in supercapacitors and electrochemical transistors have been developed using  $\text{Mo}_{1.33}\text{C}$  i-MXene nanosheets and poly(3,4-ethylenedioxothiophene): polystyrene sulfonate hybrid paste.<sup>119</sup> Indeed, MXene fiber-based supercapacitors have shown great potential in wearable electronics, because of their large surface area, suitable conductivity, and high power density.<sup>81,114</sup> However, MXene flakes may possess a non-liquid crystal structure, which renders them arduous to spin independently.<sup>81,120</sup> In one study, conductive textile was constructed through the electrostatic self-assembly between positively charged polyester fabric altered with polyethylenimine and negatively charged MXene flakes. After combining the conductive textile with conformally coated polypyrrole, they could be applied as supercapacitor electrodes with advantages of large areal capacitance, excellent rate performance, and high cycling stability without compromising its mechanical endurance.<sup>121</sup> Despite recent developments in textile electrodes for developing next-generation supercapacitors, their scalable production with multifunctionality still remains an important perplexing issue.

Notwithstanding the progress made in the synthesis of MXenes, there is still a lot of room for additional explorations to address the requirements for special applications.<sup>122</sup> Future studies ought to be undertaken in solving the challenges related to the optimization of the synthesis techniques, and the need for careful optimum consideration of several parameters to analyze the as-prepared MXenes. The chemical stability and storage of MXenes, and the modification of MXenes properties for appropriate applications by changing their composition, adopting alternative elements of "M" and "X", and modifying the surface terminal functionalities are some of the options.<sup>123,124</sup> For instance, Gogotsi *et al.*<sup>50</sup> introduced a simple electrospinning technique for fabricating MXene composite fibers using various polymers, paving a way to obtain high-performance MXene-based supercapacitor electrodes. In another study, a novel technique was introduced for enhancing the ion accessibility of MXene ( $\text{Ti}_3\text{C}_2\text{T}_x$ ) films through the femtosecond laser ablation tactic for developing high-rate MXene-based supercapacitor electrodes with higher specific capacitance along with suitable rate capability and long cycling life.<sup>125</sup> In addition, a novel strategy has been reported for large area fabrication of flexible and wearable in-plane micro-supercapacitors *via* a laser-assisted thermal paste-tear technique. The electrodes constructed from the poly(diallyldimethylammonium chloride)-mediated MXene/graphene framework exhibited excellent flexibility and mechanical stability, with high capacitance and energy density.<sup>126</sup> Chen *et al.*<sup>127</sup> introduced a dot-matrix drop-casting technique with the inherent benefits of promptness and outstanding uniformity to attain a composite as a free-standing electrode with a large specific capacitance ( $\sim 282 \text{ mF cm}^{-2}$  at  $1 \text{ mA cm}^{-2}$ ) as well as superb conductivity ( $2.3 \text{ S cm}^{-1}$ ), showing outstanding tensile strength and a porous structure.<sup>127</sup> Thus, research should be directed towards finding optimal and industrial solutions for

manufacturing novel MXene-based electrodes to develop wearable supercapacitors, with varied deformation capabilities, high capacitance, and excellent cycling stability.

Another crucial aspect in designing wearable MXene-based supercapacitors is the hybridization process, which can be contemplated as one of the promising tactics for improving the properties of MXenes in energy storage and wearable electronics.<sup>50</sup> For instance, to obtain high-performance fiber electrodes with robust mechanical strength and high electrical conductivity, MXene ( $\text{Ti}_3\text{C}_2\text{T}_x$ )/carbon nanotubes hybrid fibers were developed through a simple and scalable wet-spinning technique.<sup>128</sup> These flexible fibers exhibited improved strength along with enhanced conductivity and energy storage performance, demonstrating that hybridization can help to improve the properties of fiber-shaped supercapacitors for creating wearable and textile-based devices.<sup>128</sup> Chen *et al.*<sup>129</sup> fabricated a composite film of MXene@nitrogen-doped carbon through a vacuum filtration technique followed by annealing. It was revealed that nitrogen doping could not only improve the electrochemical activity of this composite, but the porous network could enhance the ion transport rate and the sensitivity to strain. The supercapacitor prepared from this composite film exhibited a high energy density, illustrating promising capabilities of hybrid composites in wearable electronics and energy storage devices.<sup>129</sup>

In summary, MXenes possess excellent electrical conductivity, mechanical flexibility, and a high surface area, which make them promising materials for enhancing the performances of flexible and wearable devices. Enhanced flexible and wearable devices based on MXenes utilize the unique properties of MXenes to create functional and adaptable electronic components. Several mechanisms contribute to the enhanced performance of such MXene-based devices:

### Conductivity

MXenes exhibit high electrical conductivity, allowing for efficient charge transport in flexible and wearable devices which enables the transmission of electrical signals and power delivery in these devices.<sup>130</sup>

### Mechanical flexibility

MXenes can be fabricated into thin films or incorporated into nanocomposites, offering flexibility and conformability to various substrates. This mechanical flexibility allows MXene-based devices to bend, stretch, and withstand mechanical deformations without compromising their electrical performance.<sup>131</sup>

### High surface area

MXenes possess a high surface area due to their layered structure, providing the large interface for interactions with other materials and enhancing various functionalities. The high surface area facilitates the deposition of active materials such as electrodes or sensing layers, leading to improved performance in flexible devices.<sup>12,29</sup>



## Energy storage

MXenes have excellent capacitive properties, making them ideal for energy storage applications. These materials can be used to fabricate flexible supercapacitors or energy storage devices with a high power density and long cycling stability.<sup>12,29</sup>

## Sensing capabilities

MXenes can detect various stimuli, including strain, humidity, gas, and biological analytes. By incorporating MXene-based sensing elements into wearable devices, they can be applied for real-time monitoring of physiological parameters or environmental conditions.<sup>38,39</sup>

## Hybridization

MXenes can be combined with other nanomaterials or polymers to form composites, thus exploiting advantages from the unique properties of each constituent. The hybridization can lead to enhanced mechanical properties, improved electrical conductivity, or additional functionalities in flexible and wearable devices.<sup>132,133</sup>

In addition, to improve the performance, durability, and integration of MXene-based supercapacitors for wearable applications, several challenges pertaining to the capacitance, cycling stability, synthesis difficulties, mechanical flexibility, and material integration still exist.

## Capacitance

MXenes have a high specific surface area, but their capacitance is often limited. Improving the capacitance of MXene-based supercapacitors requires optimizing the MXene composition, surface functionalization, and electrode architecture.<sup>108,134</sup>

## Cycling stability

Enhancing the cycling stability requires addressing issues like MXene restacking, electrolyte compatibility, and electrode/electrolyte interfacial stability.<sup>108</sup>

## Synthesis difficulties

Synthesizing MXenes can be challenging and typically involves complex and time-consuming processes, such as etching and delamination of precursor materials. Developing scalable, eco-friendly, and cost-effective synthesis methods for MXenes is crucial to enable their widespread applications, especially for MXene-based wearable supercapacitors.<sup>31,135-137</sup>

## Mechanical flexibility

Wearable devices require mechanical flexibility to conform to the body's shape that can withstand bending or stretching.<sup>138</sup> Achieving mechanical flexibility in MXene-based supercapacitors involves designing suitable flexible substrates, electrode materials, and binder systems.<sup>33,108</sup>

## Material integration

Wearable devices often require the integration of multiple components, embracing sensors, energy storage devices, and

communication modules.<sup>138,139</sup> The integration of MXene-based supercapacitors with other functional materials while maintaining their performance and stability is an important challenging issue that requires careful design and optimization.<sup>12,95,140</sup>

## 5. Conclusion

MXene-based supercapacitors have become a popular topic of research in recent years, particularly in wearable technologies. Researchers have developed various fabrication techniques to create flexible and wearable supercapacitors deploying MXenes/derivatives. These techniques include direct patterning of MXenes on the current collector/substrate by laser scribing, dip-coating tissue paper in MXene solution, and designing sandwich-structured electrodes. In this context, there is a vital demand for developing cost-effective, up-scalable, and simple manufacturing strategies to design wearable electronic devices. The use of MXenes in designing high-performance wearable supercapacitors with outstanding volumetric capacitance and enhanced performance has revealed promising results, in view of the unique chemical structure, versatile surface chemistry, and high electrical conductivity of MXenes. However, assembling MXene nanosheets into flexible films with wearable electronic applications still remains a crucial issue. Besides, fabricating 3D multifunctional architectures with temperature-invariant elasticity from 2D MXene nanosheets has remained exceedingly demanding. Future explorations should be conducted on cost-effective, scalable, and simple manufacturing techniques to attain wearable supercapacitors with enough flexibility along with efficient electrochemical performance and superb mechanical stability. With the mounting undertaking in the field of fiber- or textile-based energy storage devices, the next-generation of fiber-shaped electrodes endowed with mechanical robustness and high electrical conductivity can be achieved for biomedical applications. Overall, MXene-based wearable supercapacitors represent a breakthrough in biomedical engineering, offering a myriad of applications in healthcare and biotechnology. Their flexible, lightweight, and biocompatible properties make them an alluring choice for powering the wearable devices, thereby transforming the way healthcare is delivered. These supercapacitors offer several advantages for healthcare applications, including flexibility, high energy density, excellent electrochemical performance, and biocompatibility. These features make them suitable for integration into wearable devices for long-lasting power and comfortable applications. However, there are also challenges to consider, such as scalability, stability, integration with other components, and cost-effectiveness. More elaborative studies are warranted to optimize manufacturing processes, enhance stability, ensure compatibility with other components, and reduce the production costs. As ongoing research and development continue to refine MXene-based technologies, an exciting future awaits, teeming with wearable devices that enhance patient outcomes, enable remote monitoring, and revolutionize the field of biomedicine and healthcare.



## Conflicts of interest

The authors declare no conflicts of interest.

## References

- 1 X. Zhang, C. Jiang, J. Liang and W. Wu, *J. Mater. Chem. A*, 2021, **9**, 8099–8128.
- 2 J. Rehman, K. Eid, R. Ali, X. Fan, G. Murtaza, M. Faizan, A. Laref, W. Zheng and R. S. Varma, *ACS Appl. Energy Mater.*, 2022, **5**, 6481–6498.
- 3 S. Wang, J. He, Q. Li, Y. Wang, C. Liu, T. Cheng and W. Y. Lai, *Fundam. Res.*, 2022, DOI: [10.1016/j.fmre.2022.06.003](https://doi.org/10.1016/j.fmre.2022.06.003).
- 4 V. S. Bhat, A. Toghan, G. Hegde and R. S. Varma, *J. Energy Storage*, 2022, **52**, 104776.
- 5 D. Li, S. Yang, X. Chen, W.-Y. Lai and W. Huang, *Adv. Funct. Mater.*, 2021, **31**, 2107484.
- 6 S. Azizi, M. Seifi, M. T. Tournchi Moghadam, M. B. Askari and R. S. Varma, *J. Phys. Chem. Solids*, 2023, **174**, 111176.
- 7 P. Taravati Ahmad, B. Jaleh, S. Khazalpour, R. Gharehbaghi and R. S. Varma, *J. Mater. Sci.: Mater. Electron.*, 2021, **32**, 3038–3053.
- 8 A. Pullanchiyodan, R. Joy, P. Sreeram, L. R. Raphael, A. Das, N. T. M. Balakrishnan, J.-H. Ahn, A. Vlad, S. Sreejith and P. Raghavan, *Energy Adv.*, 2023, **2**, 922–947.
- 9 Y. Zhu, S. Wang, J. Ma, P. Das, S. Zheng and Z.-S. Wu, *Energy Storage Mater.*, 2022, **51**, 500–526.
- 10 A. Pullanchiyodan, L. Manjakkal, S. Dervin, D. Shakthivel and R. Dahiya, *Adv. Mater. Technol.*, 2020, **5**, 1901107.
- 11 P. Sundriyal and S. Bhattacharya, *Sci. Rep.*, 2020, **10**, 13259.
- 12 M. Hu, H. Zhang, T. Hu, B. Fan, X. Wang and Z. Li, *Chem. Soc. Rev.*, 2020, **49**, 6666–6693.
- 13 S. Iravani and R. S. Varma, *Mater. Adv.*, 2021, **2**, 2906–2917.
- 14 S. Iravani and R. S. Varma, *Nano-Micro Lett.*, 2022, **14**, 213.
- 15 S. Iravani and R. S. Varma, *Matter*, 2022, **5**, 3574–3576.
- 16 A. Zarepour, S. Ahmadi, N. Rabiee, A. Zarrabi and S. Iravani, *Nano-Micro Lett.*, 2023, **15**, 100.
- 17 X. Xu, L. Yang, W. Zheng, H. Zhang, F. Wu, Z. Tian, P. Zhang and Z. M. Sun, *Mater. Rep.: Energy*, 2022, **2**, 100080.
- 18 Y. Bao, Y. Liu, Y. Kuang, D. Fang and T. Li, *Energy Storage Mater.*, 2020, **33**, 55–61.
- 19 V. K. A. Muniraj, M. K. Srinivasa and H. D. Yoo, *Bull. Korean Chem. Soc.*, 2023, **44**, 125–136.
- 20 L.-Q. Yao, Y. Qin, X.-C. Li, Q. Xue, F. Liu, T. Cheng, G.-J. Li, X. Zhang and W.-Y. Lai, *InfoMat*, 2023, **5**, e12410.
- 21 Q. Zhao, Q. Zhu, J. Miao, P. Zhang and B. Xu, *Nanoscale*, 2019, **11**, 8442–8448.
- 22 T.-H. Chang, T. Zhang, H. Yang, K. Li, Y. Tian, J. Y. Lee and P.-Y. Chen, *ACS Nano*, 2018, **12**, 8048–8059.
- 23 Y. Wang, X. Wang, X. Li, Y. Bai, H. Xiao, Y. Liu, R. Liu and G. Yuan, *Adv. Funct. Mater.*, 2019, **29**, 1900326.
- 24 M.-Q. Zhao, X. Xie, C. E. Ren, T. Makaryan, B. Anasori, G. Wang and Y. Gogotsi, *Adv. Mater.*, 2017, **29**, 1702410.
- 25 M.-Q. Zhao, C. E. Ren, Z. Ling, M. R. Lukatskaya, C. Zhang, K. L. Van Aken, M. W. Barsoum and Y. Gogotsi, *Adv. Mater.*, 2015, **27**, 339–345.
- 26 W. Tian, A. VahidMohammadi, M. S. Reid, Z. Wang, L. Ouyang, J. Erlandsson, T. Pettersson, L. Wagberg, M. Beidaghi and M. M. Hamed, *Adv. Mater.*, 2019, **31**, 1902977.
- 27 Y.-T. Du, X. Kan, F. Yang, L.-Y. Gan and U. Schwingenschlogl, *ACS Appl. Mater. Interfaces*, 2018, **10**, 32867–32873.
- 28 X. Wang, Q. Fu, J. Wen, X. Ma, C. Zhu, X. Zhang and D. Qi, *Nanoscale*, 2018, **10**, 20828–20835.
- 29 A. K. Tareen, K. Khan, M. Iqbal, Y. Zhang, J. Long, A. Mahmood, N. Mahmood, Z. Xie, C. Li and H. Zhang, *Energy Storage Mater.*, 2022, **53**, 783–826.
- 30 B. Zazoum, A. Bachri and J. Nayfeh, *Materials*, 2021, **14**, 6603.
- 31 S. Iravani, *Ceram. Int.*, 2022, **48**, 24144–24156.
- 32 J. Zhang, S. Seyedin, Z. Gu, W. Yang, X. Wang and J. M. Razal, *Nanoscale*, 2017, **9**, 18604–18608.
- 33 Y. Wang and Y. Wang, *SmartMat*, 2023, **4**, e1130.
- 34 J. Zhang, D. Jiang, L. Liao, L. Cui, R. Zheng and J. Liu, *Chem. Eng. J.*, 2022, **429**, 132232.
- 35 A. Inman, T. Hryhorchuk, L. Bi, R. J. Wang, B. Greenspan, T. Tabb, E. M. Gallo, A. VahidMohammadi, G. Dion, A. Danielescu and Y. Gogotsi, *J. Mater. Chem. A*, 2023, **11**, 3514–3523.
- 36 D. Kasprzak, C. C. Mayorga-Martinez, O. Alduhaish and M. Pumera, *Energy Technol.*, 2023, **11**, 2201103.
- 37 V. Kedambaimoole, K. Harsh, K. Rajanna, P. Sen, M. M. Nayak and S. Kumar, *Mater. Adv.*, 2022, **3**, 3784–3808.
- 38 N. Li, J. Peng, W.-J. Ong, T. Ma, A. Arramel, P. Zhang, J. Jiang, X. Yuan and C. J. Zhang, *Matter*, 2021, **4**, 377–407.
- 39 M. Xin, J. Li, Z. Ma, L. Pan and Y. Shi, *Front. Chem.*, 2020, **8**, 297.
- 40 G. M. Karim, P. Dutta, A. Majumdar, A. Patra, S. K. Deb, S. Das, N. V. Dambhare, A. K. Rath and U. N. Maiti, *Carbon*, 2023, **203**, 191–201.
- 41 G. Zhou, X. Wang, T. Wan, C. Liu, W. Chen, S. Jiang, J. Han, Y. Yan, M.-C. Li and C. Mei, *Energy Environ. Mater.*, 2022, e12454.
- 42 Y. Wang, X. Wang, X. Li, X. Li, Y. Liu, Y. Bai, H. Xiao and G. Yuan, *Adv. Funct. Mater.*, 2021, **31**, 2008185.
- 43 Y. Li, Z. Lu, B. Xin, Y. Liu, Y. Cui and Y. Hu, *Appl. Surf. Sci.*, 2020, **528**, 146975.
- 44 P. Zhang, J. Li, D. Yang, R. A. Soomro and B. Xu, *Adv. Funct. Mater.*, 2023, **33**, 2209918.
- 45 Q. Wang, J. Liu, G. Tian and D. Zhang, *Nanoscale*, 2021, **13**, 14460–14468.
- 46 W. Yang, J. J. Byun, J. Yang, F. P. Moissinac, Y. Peng, G. Tontini, R. A. W. Dryfe and S. Barg, *Energy Environ. Mater.*, 2020, **3**, 380–388.
- 47 G. Wu, Z. Yang, Z. Zhang, B. Ji, C. Hou, Y. Li, W. Jia, Q. Zhang and H. Wang, *Electrochim. Acta*, 2021, **395**, 139141.
- 48 C. Zhu and F. Geng, *Carbon Energy*, 2021, **3**, 142–152.
- 49 S. Feng, X. Wang, M. Wang, C. Bai, S. Cao and D. Kong, *Nano Lett.*, 2021, **21**, 7561–7568.
- 50 A. S. Levitt, M. Alhabeb, C. B. Hatter, A. Sarycheva, G. Dion and Y. Gogotsi, *J. Mater. Chem. A*, 2019, **7**, 269–277.



51 T. Cheng, X. L. Yang, S. Yang, L. Li, Z.-T. Liu, J. Qu, C.-F. Meng, X.-C. Li, Y.-Z. Zhang and W.-Y. Lai, *Adv. Funct. Mater.*, 2023, **33**, 2210997.

52 M. Ghidiu, M. R. Lukatskaya, M.-Q. Zhao, Y. Gogotsi and M. W. Barsoum, *Nature*, 2014, **516**, 78.

53 X. Zhang, Y. Liu, S. Dong, J. Yang and X. Liu, *Electrochim. Acta*, 2019, **294**, 233–239.

54 C. Yang, Y. Tang, Y. Tian, Y. Luo, Y. He, X. Yin and W. Que, *Adv. Funct. Mater.*, 2018, **28**, 1705487.

55 Z. Zhang, Z. Yao, X. Zhang and Z. Jiang, *Electrochim. Acta*, 2020, **359**, 136960.

56 F. Ran, T. Wang, S. Chen, Y. Liu and L. Shao, *Appl. Surf. Sci.*, 2020, **511**, 45621–145627.

57 Q. Fu, J. Wen, N. Zhang, L. Wu, M. Zhang, S. Lin, H. Gao and X. Zhang, *RSC Adv.*, 2017, 11998–12005.

58 Z. Fan, Y. Wang, Z. Xie, D. Wang, Y. Yuan, H. Kang, B. Su, Z. Cheng and Y. Liu, *Adv. Sci.*, 2018, **5**, 1800750.

59 J. Yan, C. E. Ren, K. Maleski, C. B. Hatter, B. Anasori, P. Urbankowski, A. Sarycheva and Y. Gogotsi, *Adv. Funct. Mater.*, 2017, **27**, 1701264.

60 J. Miao, Q. Zhu, K. Li, P. Zhang, Q. Zhao and B. Xu, *J. Energy Chem.*, 2021, **52**, 243–250.

61 M. Zhu, Y. Huang, Q. Deng, J. Zhou, Z. Pei, Q. Xue, Y. Huang, Z. Wang, H. Li, Q. Huang and C. Zhi, *Adv. Energy Mater.*, 2016, **6**, 1600969.

62 H. Chen, L. Yu, Z. Lin, Q. Zhu, P. Zhang, N. Qiao and B. Xu, *J. Mater. Sci.*, 2020, **55**, 1148–1156.

63 W. Luo, Y. Wei, Z. Zhuang, Z. Lin, X. Li, C. Hou, T. Li and Y. Ma, *Electrochim. Acta*, 2022, **406**, 139871.

64 L. Li, N. Zhang, M. Zhang, X. Zhang and Z. Zhang, *Dalton Trans.*, 2019, **48**, 1747–1756.

65 K. Zhao, H. Wang, C. Zhu, S. Lin, Z. Xu and X. Zhang, *Electrochim. Acta*, 2019, **308**, 1–8.

66 Y. Wang, X. Wang, X. Li, R. Liu, Y. Bai, H. Xiao, Y. Liu and G. Yuan, *Nano-Micro Lett.*, 2020, **12**, 115.

67 H. Jiang, Z. Wang, Q. Yang, M. Hanif, Z. Wang, L. Dong and M. Dong, *Electrochim. Acta*, 2018, **290**, 695–703.

68 C. Couly, M. Alhabeb, K. L. Van Aken, N. Kurra, L. Gomes, A. M. Navarro-Suárez, B. Anasori, H. N. Alshareef and Y. Gogotsi, *Adv. Electron. Mater.*, 2018, **4**, 1700339.

69 H. Huang, H. Su, H. Zhang, L. Xu, X. Chu, C. Hu, H. Liu, N. Chen, F. Liu, W. Deng, B. Gu, H. Zhang and W. Yang, *Adv. Electron. Mater.*, 2018, **4**, 1800179.

70 K. Wang, B. Zheng, M. Mackinder, N. Baule, E. Garratt, H. Jin, T. Schuelke and Q. H. Fan, *J. Energy Storage*, 2021, **33**, 102070.

71 L. Yang, W. Zheng, P. Zhang, J. Chen, W. B. Tian, Y. M. Zhang and Z. M. Sun, *J. Electroanal. Chem.*, 2018, **830–831**, 1–6.

72 X. Li, Y. Ma, P. Shen, C. Zhang, M. Cao, S. Xiao, J. Yan, S. Luo and Y. Gao, *Adv. Mater. Technol.*, 2020, **5**, 2000272.

73 W. Luo, Y. Sun, Z. Lin, X. Li, Y. Han, J. Ding, T. Li, C. Hou and Y. Ma, *J. Energy Storage*, 2023, **62**, 106807.

74 C. Cai, Z. Wei, L. Deng and Y. Fu, *ACS Appl. Mater. Interfaces*, 2021, **13**, 54170–54184.

75 T. Kshetri, D. D. Khumujam, T. I. Singh, Y. S. Lee, N. H. Kim and J. H. Lee, *Chem. Eng. J.*, 2022, **437**, 135338.

76 R. Ma, X. Zhang, J. Zhuo, L. Cao, Y. Song, Y. Yin, X. Wang, G. Yang and F. Yi, *ACS Nano*, 2022, **16**, 9713–9727.

77 H. Hu, Z. Bai, B. Niu, M. Wu and T. Hua, *J. Mater. Chem. A*, 2018, **6**, 14876–14884.

78 S. Xu, G. Wei, J. Li, Y. Ji, N. Klyui, V. Izotov and W. Han, *Chem. Eng. J.*, 2017, **317**, 1026–1036.

79 J. V. Vaghasiya, C. C. Mayorga-Martinez, J. Vyskočil, Z. Sofer and M. Pumera, *Adv. Funct. Mater.*, 2020, **30**, 2003673.

80 J. Li, J. Chen, H. Wang and X. Xiao, *ChemElectroChem*, 2021, **8**, 648–655.

81 W. Yu, Y. Li, B. Xin and Z. Lu, *Fibers Polym.*, 2022, **23**, 2994–3001.

82 Q. Yang, Z. Xu, B. Fang, T. Huang, S. Cai, H. Chen, Y. Liu, K. Gopalsamy, W. Gao and C. Gao, *J. Mater. Chem. A*, 2017, **5**, 22113–22119.

83 M. Hu, Z. Li, G. Li, T. Hu, C. Zhang and X. Wang, *Adv. Mater. Technol.*, 2017, **2**, 1700143.

84 J. S. Heo, J. Eom, Y.-H. Kim and S. K. Park, *Small*, 2018, **14**, 1703034.

85 Q. Chen, Q. Gao, X. Wang, D. W. Schubert and X. Liu, *Composites, Part A*, 2022, **155**, 106838.

86 X. Zheng, P. Wang, X. Zhang, Q. Hu, Z. Wang, W. Nie, L. Zou, C. Li and X. Han, *Composites, Part A*, 2022, **152**, 106700.

87 X. Zheng, Y. Wang, W. Nie, Z. Wang, Q. Hu, C. Li, P. Wang and W. Wang, *Composites, Part A*, 2022, **158**, 106985.

88 X. Zheng, J. Shen, Q. Hu, W. Nie, Z. Wang, L. Zou and C. Li, *Nanoscale*, 2021, **13**, 1832–1841.

89 J. V. Vaghasiya, C. C. Mayorga-Martinez, Z. Sofer and M. Pumera, *ACS Appl. Mater. Interfaces*, 2020, **12**, 53039–53048.

90 J. Ma, Z. Cui, Y. Du, J. Zhang, C. Sun, C. Hou and N. Zhu, *Adv. Fiber Mater.*, 2022, **4**, 1535–1544.

91 Y. Song, D. Mukasa, H. Zhang and W. Gao, *Acc. Mater. Res.*, 2021, **2**, 184–197.

92 M. Zhao, Y. Li, F. Lin, Y. Xu, L. Chen, W. Jiang, T. Jiang, S. Yang and Y. Wang, *J. Mater. Chem. A*, 2020, **8**, 1829–1836.

93 C. Cai, W. Zhou and Y. Fu, *Chem. Eng. J.*, 2021, **418**, 129275.

94 Y. Lu, Z. Lou, K. Jiang, D. Chen and G. Shen, *Mater. Today Nano*, 2019, **8**, 100050.

95 Q. Jiang, C. Wu, Z. Wang, A. C. Wang, J.-H. He, Z. L. Wang and H. N. Alshareef, *Nano Energy*, 2018, **45**, 266–272.

96 X. Li, Y. Ma, Y. Yue, G. Li, C. Zhang, M. Cao, Y. Xiong, J. Zou, Y. Zhou and Y. Gao, *Chem. Eng. J.*, 2022, **428**, 130965.

97 S. Abdolhosseinzadeh, R. Schneider, A. Verma, J. Heier, F. Nüesch and C. J. Zhang, *Adv. Mater.*, 2020, **32**, 2000716.

98 Y. Cai, J. Shen, G. Ge, Y. Zhang, W. Jin, W. Huang, J. Shao, J. Yang and X. Dong, *ACS Nano*, 2018, **12**, 56–62.

99 Q. Yi, X. Pei, P. Das, H. Qin, S. W. Lee and R. Esfandyarpour, *Nano Energy*, 2022, **101**, 107511.

100 S. Zheng, H. Wang, P. Das, Y. Zhang, Y. Cao, J. Ma, S. Liu and Z.-S. Wu, *Adv. Mater.*, 2021, **33**, 2005449.

101 N. Driscoll, B. Erickson, B. B. Murphy, A. G. Richardson, G. Robbins, N. V. Apollo, G. Mentzelopoulos, T. Mathis, K. Hantanasisirisakul, P. Bagga, S. E. Gullbrand,



M. Sergison, R. Reddy, J. A. Wolf, H. I. Chen, T. H. Lucas, T. Dillingham, K. A. Davis, Y. Gogotsi, J. D. Medaglia and F. Vitale, *Sci. Transl. Med.*, 2021, **13**, eabf8629.

102 S. Nahirniak, A. Ray and B. Saruhan, *Batteries*, 2023, **9**, 126.

103 Y. Liu, H. Zhou, W. Zhou, S. Meng, C. Qi, Z. Liu and T. Kong, *Adv. Energy Mater.*, 2021, **11**, 2101329.

104 C. Li, S. Wang, X. Wang, W. Bai, H. Sun, F. Pan, Y. Chi and Z. Wang, *ACS Mater. Lett.*, 2023, **5**, 2084–2095.

105 Y. Ma, D. Zhang, Z. Wang, H. Zhang, H. Xia, R. Mao, H. Cai and H. Luan, *ACS Appl. Mater. Interfaces*, 2023, **15**, 29413–29424.

106 J. Ma, K. Yang, Y. Jiang, L. Shen, H. Ma, Z. Cui, Y. Du, J. Lin, J. Liu and N. Zhu, *Cell Rep. Phys. Sci.*, 2022, **3**, 100908.

107 J. V. Vaghasiya, C. C. Mayorga-Martinez and M. Pumera, *npj Flexible Electron.*, 2023, **7**, 26.

108 B. Shen, R. Hao, Y. Huang, Z. Guo and X. Zhu, *Crystals*, 2022, **12**, 1099.

109 M. R. Islam, S. Afroj, K. S. Novoselov and N. Karim, *Adv. Sci.*, 2022, **9**, 2203856.

110 J. Yin, S. Wang, A. Di Carlo, A. Chang, X. Wan, J. Xu, X. Xiao and J. Chen, *Med-X*, 2023, **1**, 3.

111 J. Luo, S. Gao, H. Luo, L. Wang, X. Huang, Z. Guo, X. Lai, L. Lin, R. K. Y. Li and J. Gao, *Chem. Eng. J.*, 2021, **406**, 126898.

112 W. Shao, M. Tebyetekerwa, I. Marriam, W. Li, Y. Wu, S. Peng, S. Ramakrishna, S. Yang and M. Zhu, *J. Power Sources*, 2018, **396**, 683–690.

113 X. Jian, H. Li, H. Li, Y. Li and Y. Shang, *Carbon*, 2021, **172**, 132–137.

114 Z. Guo, Z. Lu, Y. Li and W. Liu, *Adv. Mater. Interfaces*, 2022, **9**, 2101977.

115 A. S. Etman, J. Halim and J. Rosen, *Nano Energy*, 2021, **88**, 106271.

116 Y. Li, B. Xin, Z. Lu, X. Zhou, Y. Liu and Y. Hu, *Int. J. Energy Res.*, 2021, **45**, 9229–9240.

117 R. Wang, S. Luo, C. Xiao, Z. Chen, H. Li, M. Asif, V. Chan, K. Liao and Y. Sun, *Electrochim. Acta*, 2021, **386**, 138420.

118 A. A. P. R. Perera, K. A. U. Madhushani, B. T. Punchihewa, A. Kumar and R. K. Gupta, *Materials*, 2023, **16**, 1138.

119 L. Qin, J. Jiang, L. Hou, F. Zhang and J. Rosen, *J. Mater. Chem. A*, 2022, **10**, 12544–12550.

120 J. Zhang, S. Uzun, S. Seyedin, P. A. Lynch, B. Akuzum, Z. Wang, S. Qin, M. Alhabeb, C. E. Shuck, W. Lei, E. C. Kumbur, W. Yang, X. Wang, G. Dion, J. M. Razal and Y. Gogotsi, *ACS Cent. Sci.*, 2020, **6**, 254–265.

121 X. Li, J. Hao, R. Liu, H. He, Y. Wang, G. Liang, Y. Liu, G. Yuan and Z. Guo, *Energy Storage Mater.*, 2020, **33**, 62–70.

122 U. U. Rahman, M. Humayun, U. Ghani, M. Usman, H. Ullah, A. Khan, N. M. El-Metwaly and A. Khan, *Molecules*, 2022, **27**, 15.

123 Z. U. D. Babar, B. D. Ventura, R. Velotta and V. Iannotti, *RSC Adv.*, 2022, **12**, 19590–19610.

124 A. Bhat, S. Anwer, K. S. Bhat, M. I. H. Mohideen, K. Liao and A. Qurashi, *npj 2D Mater. Appl.*, 2021, **5**, 61.

125 X. Zheng, *J. Alloys Compd.*, 2022, **899**, 163275.

126 K. Chen, C. Gao, B. Lu, X. Jin, C. Shao, J. Wang, W. Wu, L. Qu and Y. Zhao, *J. Power Sources*, 2022, **532**, 231346.

127 W. Chen, M. Luo, K. Yang, C. Liu, D. Zhang and X. Zhou, *Chem. Eng. J.*, 2021, **423**, 130242.

128 X. Zhao, J. Zhang, K. Lv, N. Kong, Y. Shao and J. Tao, *Carbon*, 2022, **200**, 38–46.

129 A. Chen, C. Wang, O. A. Abu Ali, S. F. Mahmoud, Y. Shi, Y. Ji, H. Algadi, S. M. El-Bahy, M. Huang, Z. Guo, D. Cui and H. Wei, *Composites, Part A*, 2022, **163**, 107174.

130 A. Lipatov, A. Goad, M. J. Loes, N. S. Vorobeva, J. Abourahma, Y. Gogotsi and A. Sinitskii, *Matter*, 2021, **4**, 1413–1427.

131 S. Mazhar, A. A. Qarni, Y. U. Haq, Z. Ul Haq and I. Murtaza, *Ceram. Int.*, 2020, **46**, 12593–12605.

132 D. Parajuli, N. Murali, K. C. Devendra, B. Karki, K. Samatha, A. A. Kim, M. Park and B. Pant, *Polymers*, 2022, **14**, 3433.

133 C. Gu, C. Lu, Y. Gao, P. Tan, S. Peng, X. Liu and L. Sun, *Inorg. Chem.*, 2021, **60**, 1380–1387.

134 S. Alam, F. Fiaz, M. Ishaq Khan, M. Zahir Iqbal, Z. Ahmad and H. H. Hegazy, *J. Alloys Compd.*, 2023, **961**, 171007.

135 T. Amrillah, C. A. Che Abdullah, A. Hermawan, F. N. Indah Sari and V. N. Alviani, *Nanomaterials*, 2022, **12**, 4280.

136 F. Bu, M. M. Zagho, Y. Ibrahim, B. Ma, A. Elzatahry and D. Zhao, *Nanotoday*, 2020, **30**, 100803.

137 K. R. G. Lim, M. Shekhirev, B. C. Wyatt, B. Anasori, Y. Gogotsi and Z. W. Seh, *Nat. Synth.*, 2022, **1**, 601–614.

138 B. Wang and A. Facchetti, *Adv. Mater.*, 2019, **31**, 1901408.

139 Kenry, J. C. Yeo and C. T. Lim, *Microsyst. Nanoeng.*, 2016, **2**, 16043.

140 S. Mallakpour, V. Behranvand and C. M. Hussain, *Ceram. Int.*, 2021, **47**, 26585–26597.

